United States Food and Drug Administration. The efficacy of MPC polymer as a biomaterial is well established [15–17].

Based on the biocompatibility and hydrophilicity of MPC polymer, we have been developing new artificial joints with highly lubricated bearing surfaces produced by photo-induced radical graft polymerization. This technique grafts MPC directly to CLPE, forming C–C covalent bonds between the CLPE substrate and the MPC polymer. In this study, we investigated the effects of this photo-induced radical graft polymerization technique on the physical, mechanical and tribological properties of CLPE-*g*-MPC.

Materials and methods

Chemicals and MPC graft polymerization

Benzophenone and acetone were purchased from Wako Pure Chemical Industries, Ltd (Osaka, Japan). MPC was synthesized industrially using the method of Ishihara, et al. [13] and was supplied by AI Bio-Chips Co., Ltd (Tokyo, Japan).

Compression-molded UHMWPE (GUR1020 resin, Poly Hi Solidur Inc., IN, USA) bar stock was gamma-irradiated with 50 kGy in N_2 gas and annealed at 120°C in N_2 gas for cross-linking. The CLPE specimens were machined from this bar stock after cooling. They were immersed for 30 sec in an acetone solution containing 10 mg/mL benzophenone and then dried in the dark to remove acetone at room temperature [18]. The amount of benzophenone adsorbed on the surface was 3.5×10^{-11} mol/cm^2 by ultraviolet spectroscopy according to the previous study [19]. The MPC was dissolved into degassed pure water to a concentration of 0.5 mol/L. CLPE specimens coated with benzophenone were immersed in the aqueous MPC solution. Photo-induced graft polymerization on the CLPE surface was carried out with ultraviolet irradiation of 5 mW/cm^2 for 10 to 360 min at 60°C using a Toshiba D-35 filter to pass only ultraviolet of 350 ± 50 nm wavelength. After the polymerization, the CLPE-*g*-MPC specimens were removed, washed with pure water and ethanol, and dried.

Surface analysis by FT-IR/ATR and XPS

The functional group vibrations of the CLPE and CLPE-*g*-MPC (90 min irradiation) surfaces were examined by Fourier-transform infrared (FT-IR) spectroscopy with attenuated total reflection (ATR) equipment. CLPE and CLPE-*g*-MPC spectra were obtained in 32 scans over the range of 800 to 2000 cm^{-1} with an FT-IR analyzer (FT/IR615, JASCO Co. Ltd., Tokyo, Japan) at a resolution of 4.0 cm^{-1}.

The surface elemental composition of CLPE was analyzed before and after MPC grafting for 90 min by X-ray photoelectron spectroscopy (XPS). The XPS spectra were obtained on an AXIS-HSi165 (KRATOS ANALYTICAL Ltd., UK) equipped with Mg–Kα radiation source biased at 15 kV at the anode. The take-off angle of photoelectrons was kept at 90°.

Surface wettability observation by spray method

The spray method is based on the wetting response of the surface of a cup when exposured to a distilled water mist for a short period [20]. The entire bearing surfaces of CLPE and CLPE-*g*-MPC (23 and 90 min irradiation) cups were uniformly exposed to 15 mL of water mist. The appearance of the cup surfaces was evaluated in terms of wettability within 10 sec after spraying. Ratio of surface area covered by water (water-covered ratio) was determined by using the Win-Roof image processing system (Mitani Corporation Inc., Fukui, Japan).

Evaluation of physical and mechanical properties

The density, swelling ratio, network chain density, molecular weight between cross-links and cross-link density of CLPE and CLPE-*g*-MPC with irradiation for 90 min were evaluated according to the methods previously reported [21]. The CLPE and CLPE-*g*-MPC specimens ($23 \times 23 \times 1$ mm^3) were weighed (approximately 0.5 g, V_1), allowed to swell for 72 h in *p*-xylene containing 0.5 wt% 2-*t*-butyl-4-methylphenol at 130 °C, and were then reweighed (V_2). After reweighing, specimens were immersed in acetone, dried at 60 °C under vacuum, and reweighed (V_3). The swelling ratio, q, was determined from the weight gain and densities of the polyethylene and xylene, and the physical properties were calculated as follows.

(a) Swelling ratio, q

$$q = V_2 / V_3 \tag{1}$$

(b) Network chain density, v^*

$$v* = In\,(1 - q^1) + q^1 + \chi q^2 / V_1\,(q^{-2/3} - 0.5q^{-1})$$
$$V_1 = 136\ mL/mol\ ,\ \chi = 0.37\ (polyethylene) \tag{2}$$

(c) Molecular weight between cross-links, M_c

$$M_c = 1 / \bar{M}c = \mathrm{V}v*$$
$$V = 1 / specimen\ density \tag{3}$$

(d) Cross-link density, *XLD*

$$XLD = M_0/\bar{M}C \qquad M_0 = 14\ (polyethylene) \tag{4}$$

The mechanical properties of CLPE and CLPE-*g*-MPC with irradiation for 90 min were evaluated with tensile, impact, and creep deformation tests, as well as a shore hardness D measurement. Tensile testing was performed according to ASTM standard D638 using a type 4 tensile bar specimen and a crosshead speed of 50 mm/min. A double-notched (notch depth = 4.57 ± 0.08 mm) Izod impact strength test was performed to ASTM standard F648. Ten specimens were used in each tests. Creep deformation was measured by applying a constant load (113 kgf for 24 h) to a specimen, then measuring the height displacement, according to the ASTM D621 test method. Shore hardness D was measured according to the ASTM D2240 test method.

For all the test groups, the results derived from each experiment were expressed as mean values and the standard deviation. The statistical significance ($p < 0.05$) was judged by the Student's *t*-test.

TEM observation of cross section of CLPE-*g*-MPC

A cross section of the MPC polymer layer on the CLPE-*g*-MPC (90 min irradiation) surface before and after the hip joint simulator test was observed with a transmission electron microscope (TEM). Prior to observation, specimens were embedded in epoxy resin, stained in ruthenium oxide vapor at room temperature, and sliced into ultra-thin films. The specimen after the hip joint simulator test was coated with gold by sputter coater (JFC 1500, JEOL, Ltd., Tokyo, Japan) before embedding in resin. A JEM-1010 (JEOL, Ltd., Tokyo, Japan) was used for the TEM observation at an acceleration voltage of 100 kV.

Hip joint simulator test

The CLPE-*g*-MPC cups (26 mm inner diameter and 52 mm outer diameter) for testing in the hip joint simulator were gamma-ray sterilized under N_2 gas.

Friction torque between the CLPE-*g*-MPC cup and a 26 mm Co–Cr–Mo alloy femoral head (Japan Medical Materials Corp., Japan) was measured using a 2-station hip joint simulator (Kobe Steel, Ltd., Kobe, Japan). Measurements were performed with distilled water as lubricant, a loading of 280 kgf and a swing distance of 80 mm with a period of 1 Hz.

The in vitro wear test was performed using a 12-station hip joint simulator (MTS system Corp., MN, USA). A mixture of 25% bovine serum, 20 mM/L of ethylene diamine tetraacetic acid (EDTA), and 0.1% sodium azide was used as lubricant, according to the ISO 14242-1 standard. A load simulating a physiologic loading curve with double peaks of 183 and 280 kgf load was added with a period of 1 Hz. The wear was measured by a gravimetric method. The cup weights were measured every 0.5×10^6 cycles. The acetabular component was tested with a 26 mm Co–Cr–Mo alloy femoral head (Japan Medical Materials Corp., Japan). Testing then continued until a total of 3.0×10^6 cycles were completed.

Results

Figure 1 shows the FT-IR/ATR spectra of CLPE and CLPE-*g*-MPC. A transmission absorption peak was observed at 1460 cm^{-1} for both CLPE and CLPE-*g*-MPC. This peak is attributed mainly to the methylene chain in the CLPE substrate and MPC graft polymer. However, transmission absorptions at 1240, 1080 and 970 cm^{-1} were observed only for the CLPE-*g*-MPC. These peaks are due to the phosphate group in the MPC unit. Similarly, the transmission absorption at 1720 cm^{-1} observed for CLPE-*g*-MPC can only correspond to the carbonyl in the MPC unit.

Figure 2 shows the XPS spectra (N_{1s} and P_{2p}) of CLPE and CLPE-*g*-MPC. In the N_{1s} and P_{2p} spectra, clear peaks were observed only for CLPE-*g*-MPC. Peaks at 403 and 134 eV were assigned to the $-N^+(CH_3)_3$ and phosphate groups, respectively. These peaks were characteristic of the phosphorylcholine in the MPC unit. Table 1 summarizes the elemental composition of the untreated CLPE and the CLPE-*g*-MPC surfaces with various ultraviolet-ray irradiation times during polymerization. The content of nitrogen and phosphorous in the CLPE-*g*-MPC surface was increased to 5.1 and 5.2, respectively, with polymerization time. The elemental composition of the CLPE-*g*-MPC surface with a polymerization time of 90 min was almost

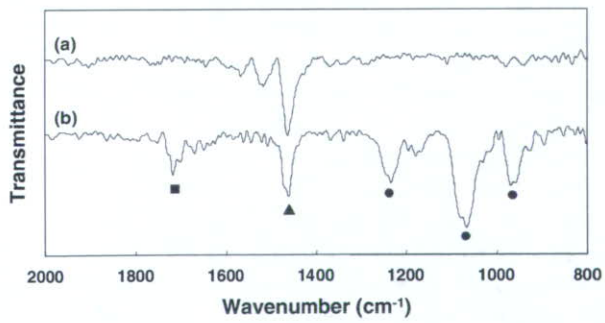

Fig. 1 FT-IR/ATR spectra of CLPE-*g*-MPC. (**a**) CLPE (untreated), (**b**) CLPE-*g*-MPC. •: P–O, ▲: CH_2, ■: C=O

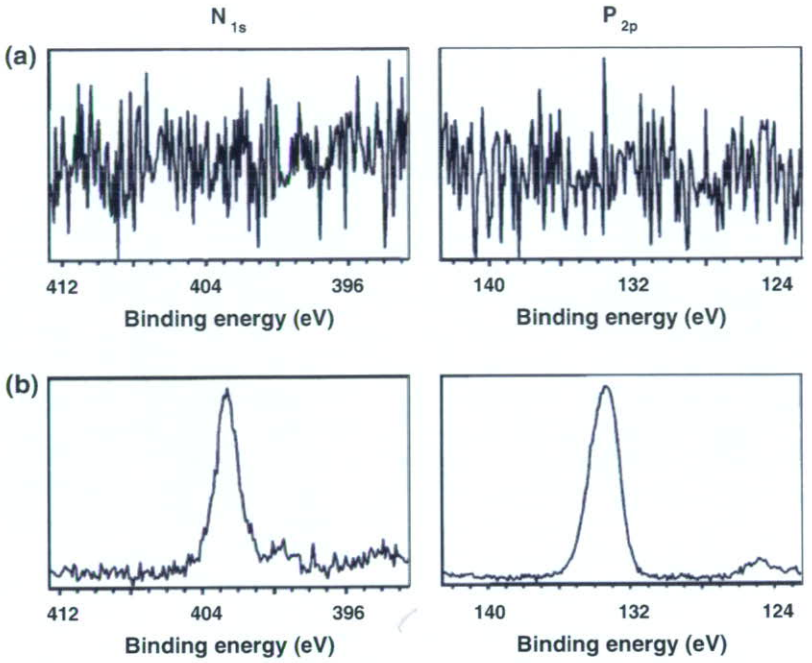

Fig. 2 XPS spectra of CLPE-*g*-MPC. (**a**) CLPE (untreated), (**b**) CLPE-*g*-MPC

Table 1 Surface elemental composition (%) of CLPE-*g*-MPC with various photo-polymerization times

Polymerization time (min)	C	O	N	P
0 (untreated CLPE)	99.6	0.4	0.0	0.0
12	96.6	3.4	0.0	0.0
23	78.5	17.0	1.9	2.7
45	60.4	30.2	4.1	5.3
90	61.8	27.9	5.1	5.2
MPC polymer*	57.9	31.6	5.3	5.3

*: Theoretical elemental composition of MPC polymer

equivalent to the theoretical elemental composition (N = 5.3, P = 5.3) of MPC polymer.

Figure 3 shows optical microscope images of moistened CLPE-*g*-MPC surfaces that were produced by various photo-irradiation times during polymerization. The surface image progressively alters from a hydrophobic surface to a hydrophilic one as polymerization time increases. On an untreated CLPE surface after spraying with water mist, typical hydrophobic behavior was observed, including the formation of many water droplets (Fig. 3a). In contrast, on the CLPE-*g*-MPC surface hydrophilic behavior was observed, characterized by a thin film of water (Fig. 3c).

The physical properties of CLPE and CLPE-*g*-MPC including density and swelling ratio are summarized in Table 2. It is generally said that energy irradiation to polyethylene causes a decrease in the swelling ratio. However, all of the bulk physical properties of CLPE and CLPE-*g*-MPC that were examined in this study differed little ($p < 0.05$) between the two materials.

The tensile yield strength, impact strength, creep deformation and shore hardness D of CLPE and CLPE-*g*-MPC are shown in Table 3. Tensile yield strength, impact strength and shore hardness D did not differ significantly ($p \leq 0.05$) between CLPE and CLPE-*g*-MPC, and both CLPE and CLPE-*g*-MPC met ASTM requirements (F648).

Figure 4 shows a TEM image of a cross section of CLPE-*g*-MPC. A grafted MPC polymer layer about 100 nm thick was observed on the CLPE substrate (Fig. 4b). Lamellae on the order of 100–400 nm long and 10–20 nm thick were observed in the CLPE substrate regardless of irradiation, and the lamellae were especially thin near the surface.

Table 4 shows the friction coefficient and the wear rate of the MPC polymer grafted CLPE cup in the hip joint simulator test. The friction coefficients of the untreated CLPE cups and the CLPE-*g*-MPC cups were 0.0075 and 0.0009, respectively. The CLPE-*g*-MPC cups reduced 88% in the friction coefficient compared with untreated CLPE cups, showed a high lubricity. We calculated the wear rate between 2.5×10^6 and 3.0×10^6 cycles. The wear rate of CLPE cups showed 3.12 mg/10^6 cycles. In contrast, the CLPE-*g*-MPC cups showed the reduction in wear to an essentially zero of −1.43 mg/10^6 cycles. The volumetric change was then calculated from the weight loss over time. In this study, the weight loss was calculated without considering the effect of water absorption.

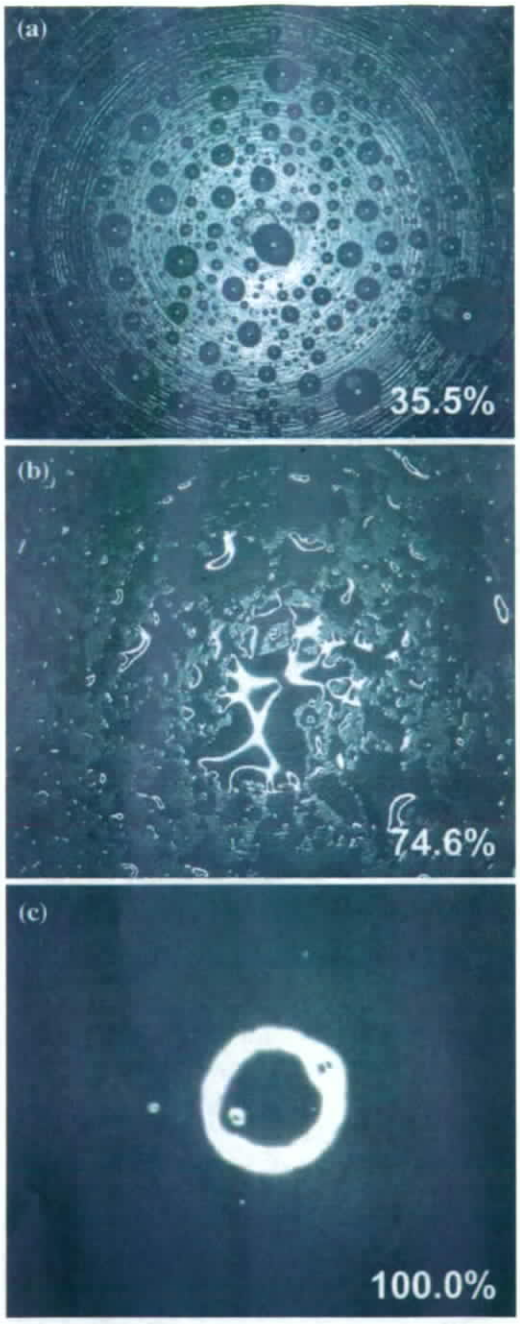

Fig. 3 Optical microscope images of CLPE-*g*-MPC cup surface with various photo-polymerization times. (**a**) 0 min (untreated CLPE), (**b**) 23 min and (**c**) 90 min. The water-covered ratio (%) is also shown. The white ring in (**c**) is due to the reflection of the light used in photography

Discussion

We have developed an artificial hip joint that uses CLPE-*g*-MPC on the bearing surface, with the goal of reducing wear and avoiding bone resorption. In this study, we investigated the effects of photo-induced radical graft polymerization technique on properties of the CLPE-*g*-MPC, and this report discusses the characteristics of the MPC polymer layer and the properties of the CLPE substrate.

After 3.0×10^6 cycles of the hip joint simulator test, we confirmed that the CLPE-*g*-MPC cups showed a quite low wear rate compared with untreated CLPE. Since MPC is a highly hydrophilic compound, and poly(MPC) is water-soluble, the water-wettability of the CLPE-*g*-MPC surface was greater than that of a CLPE surface due to the poly(MPC) chains, as shown in Fig. 3. It was observed that the CLPE-*g*-MPC surface supported a thin film of water. Consequently, the artificial hip joint bearing with an CLPE-*g*-MPC surface had high lubricity. The reduction in friction is assumed to have contributed to the improvement of anti-wear properties that was observed [22]. However, different processes such as migration of low molecular weight compounds, rotation of flexible polymer chains, inter- and intra-molecular rearrangements, and adhesion of contaminant particles, may take place at different rates depending on materials and ambient conditions [23]. Various factors such as type of bearing material, surface roughness, homogeneity of the surface and chemical composition affect the lubricity of the artificial joint [24]. In CLPE-*g*-MPC, the lubricity can change depending on the ambient conditions in vitro and in vivo. The bearing surface of the artificial hip joint with MPC polymer is assumed to have a structure similar to an artificial cell membrane, meaning this new concept artificial hip joint mimics the natural joint cartilage in vivo. To ensure the long-term retention of the benefits of this MPC polymer, we used photo-induced radical graft polymerization technique, to produce C–C covalent bonding between a carbon atom of the CLPE and the end-group of an MPC polymer chain. The results clearly show that the crystalline structure, physical and mechanical properties of the CLPE substrate were minimally changed, if at all, even after MPC grafting [25]. This indicates that photo-induced radical graft polymerization does not affect the properties of the CLPE substrate [18]. Retaining the properties of the CLPE substrate unchanged is very important in clinical use, because the CLPE cup acts not only as a bearing material but also as a structural material in the artificial hip joint system. Generally, increased cross-linking in the CLPE degrades its mechanical properties, producing a trade-off between wear-resistance and mechanical properties [5, 26]. It is desirable to reduce wear while maintaining the mechanical properties necessary for proper in vivo function. The advantage of photo-induced radical graft polymerization comes from the fact that the grafted MPC polymer gave a high lubricity only on the surface, and had no effect on the bulk properties of the CLPE substrate.

Table 2 Physical properties of CLPE-*g*-MPC

Sample	Density (g/cm^3)	Swelling ratio	Network chain density ($\times 10^3$ mol/ml)	M.W. between Cross-links (g/mol)	Cross-link density (mol%)
CLPE	0.944 (0.002)	2.99 (0.11)	0.437 (0.043)	2165 (214)	0.65 (0.06)
CLPE-*g*-MPC	0.943 (0.001)	2.94 (0.10)	0.459 (0.044)	2069 (186)	0.68 (0.07)

The standard deviation is in parentheses

Table 3 Mechanical properties of CLPE-*g*-MPC

Sample	Yield strength (MPa)	Impact strength (kJ/m^2)	Creep deformation (%)	Hardness (shore D)
CLPE	23.2 (0.4)	75.0 (1.4)	0.89 (0.17)	68.2 (0.9)
CLPE-*g*-MPC	23.1 (0.5)	77.0 (1.9)	0.63 (0.40)	68.4 (0.5)

The standard deviation is in parentheses

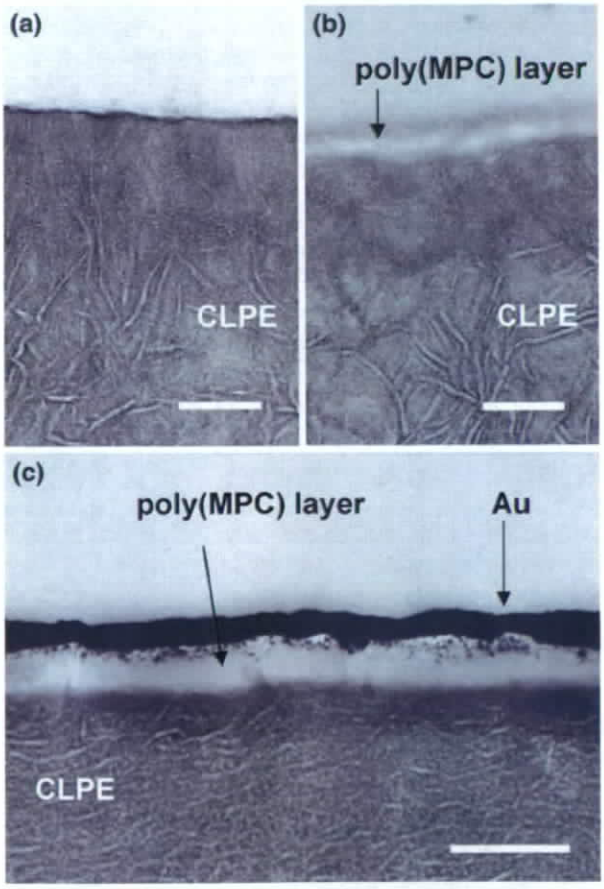

Fig. 4 Cross-sectional TEM images of CLPE-*g*-MPC. (**a**) CLPE (untreated), (**b**) CLPE-*g*-MPC before simulator test and (**c**) CLPE-*g*-MPC after a 3×10^6 cycle simulator test. Bar; 200 nm

After 3.0×10^6 cycles in the hip joint simulator test, the wear rate of CLPE-*g*-MPC cups remained low. The cross-sectional TEM image of the CLPE-*g*-MPC bearing surface after 3.0×10^6 cycles of the hip simulator test (Fig. 4c) showed that most of the bearing surface was covered by the MPC polymer layer even after the hip simulator test. In other words, the CLPE-*g*-MPC cups showed little wear on inspection, supporting the quite low wear observed in the hip joint simulator test.

Table 4 Tribological properties of CLPE-*g*-MPC

Sample	Friction coefficient	Wear rate ($mg/10^6$ cycles)
CLPE	0.0075	3.12
CLPE-*g*-MPC	0.0009	−1.43

On the CLPE-*g*-MPC surface, the nitrogen and phosphorus attributed to the phosphorylcholine in the MPC units increased with increasing polymerization time. This indicates that the density of the grafted MPC polymer can be controlled by the polymerization time, since the number of polymer chains produced in a radical polymerization is generally proportional to the photo-irradiation time. The elemental composition obtained by XPS (N = 5.1, P = 5.2) of the CLPE-*g*-MPC surface with a polymerization time of 90 min was almost equivalent to the theoretical elemental composition of MPC polymer. Therefore, the entire surface of the CLPE was assumed to be coated with an MPC polymer layer.

However, the area observed by the X-ray spot (approximately $400 \times 800\ \mu m^2$) in XPS was quite limited. As a supplementary probe to examine the MPC polymer layer, wettability measurement of cups should be performed on many separate areas on the cups. The wettability measurement of a surface is readily performed in the laboratory on well defined, homogeneous, smooth and planar surfaces of prepared specimens. In the case of artificial hip joint cups, for which non-destructive measurements are usually required (and where excision of material samples is usually undesirable), these conditions do not exist and measurement with high precision is a difficult task. Hence,

we evaluated wettability of CLPE-*g*-MPC cup by the spray method, because this method can be used non-destructively on large areas.

Since CLPE-*g*-MPC reduces the production of wear particles and bone-resorptive responses, periprosthetic osteolysis could be eliminated [12]. Based on the mechanical, tribological and biological advantages, we confidently expect CLPE-*g*-MPC be used in the next-generation of artificial hip joint systems.

Conclusions

In this study, effects of a photo-induced radical graft polymerization technique on physical, mechanical and tribological properties of CLPE-*g*-MPC were investigated. The crystalline structure, physical and mechanical properties of the CLPE substrate were unchanged after the addition of a layer of MPC polymer by photo-polymerization. However, CLPE-*g*-MPC cups reduced 88% in the friction coefficient compared with untreated CLPE cups. After 3.0×10^6 cycles in the hip joint simulator test, the wear rate of CLPE-*g*-MPC cups remained low. We concluded that the advantage of this photo-induced radical graft polymerization technique was that the grafted MPC polymer layer produces high lubricity while only affecting the surface, and has no effect on the properties of the CLPE substrate.

Acknowledgements This work was supported by a Grant-in-Aid for Scientific Research from the Japanese Ministry of Education, Culture, Sports, Science and Technology (#15390449), and a Health and Welfare Research Grant for Translational Research from the Japanese Ministry of Health, Labour and Welfare. The authors also express special thank to Dr. Fumiaki Miyaji, Mr. Yoshiki Ando and Mr. Takatoshi Miyashita (Japan Medical Materials Corp., Japan) for their excellent technical assistance.

References

1. W. H. HARRIS, *Clin. Orthop.* **311** (1995) 46
2. A. KOBAYASHI, M. A. FREEMAN, W. BINEFIELD, Y. KADOYA, T. YAMAC, N. AL-SAFFER, G. SCOTT and P. A. REVELL, *J. Bone Joint Surg.* **79**(5) (1997) 844
3. D. H. SOCHART, *Clin. Orthop.* **363** (1999) 135
4. O. K. MURATOGLU, A. MARK, D. A. VITTETOE, W. H. HARRIS and H. E. RUBASH, *J. Bone Joint Surg.* **85A** (2003) 7
5. H. MCKELLOP, F. W. SHEN, B. LU, P. CAMPBELL and R. SALOVEY, *J. Orthop. Res.* **17**(2) (1999) 157
6. O. K. MURATOGLU, C. R. BRAGDON, D. O. O'CONNOR, M. JASTY and W. H. HARRIS, J. Arthroplasty 16 (2001) 149
7. D. W. MANNING, P. P. CHIANG, J. M. MARTELL, J. O. GALANTE and W. H. HARRIS, *Orthop. Res. Soc.* (2004) 1478
8. G. DIGAS, J. KÄRRHOLM, J. THANNER, H. MALCHAU and P. HERBERTS, *Clin. Orthop. Relat. Res.* **417** (2003) 126
9. C. HEICEL, M. SILVA, M. A. DELA ROSA and T. P. SCHMALZRIED, *J. Bone Joint Surg. Am.* **86**(4) (2004) 748
10. J. M. MARTELL, J. J. VERNER and S. J. INCAVO, *J. Arthroplasty* **18**(7) (2003) 55
11. H. OONISHI, S. C. KIM, Y. TAKAO, M. KYOMOTO, M. IWAMOTO and M. UENO, *J. Arthroplasty* **21**(7) (2006) 944
12. T. MORO, Y. TAKATORI, K. ISHIHARA, T. KONNO, Y. TAKIGAWA, T. MATSUSHITA, U. I. CHUNG, K. NAKAMURA and H. KAWAGUCHI, *Nature Mater.* **3** (2004) 829
13. K. ISHIHARA, R. ARAGAKI, T. UEDA, A. WATANABE and N. NAKABAYASHI, *J. Biomed. Mater. Res.* **24** (1990) 1069
14. K. ISHIHARA, N. P. ZIATS, B. P. TIERNEY, N. NAKABAYASHI and J. M. ANDERSON, *J. Biomed. Mater. Res.* **25**(11) (1991) 1397
15. K. J. KUIPER and J. E. NORDREHAUG, *Am. J. Cardiol.* **85** (2000) 698
16. M. GALLI, L. SOMMARIVA, F. PRATI, S. ZERBONI, A. POLITI, R. BONATTU, S. MAMELI, E. BUTTI, A. PAGANO and G. FERRARI, *Cathet. Cardiovasc. Intervent.* **53** (2001) 182
17. A. L. LEWIS, L. A. TOLHURST and P. W. STRATFORD, *Biomaterials* **23** (2002) 1697
18. K. ISHIHARA, Y. IWASAKI, S. EBIHARA, Y. SHINDO and N. NAKABAYASHI, *Colloids Surf. B, Biointerfaces* **18** (2000) 325
19. K. ISHIHARA, T. UEDA and N. NAKABAYASHI, *Polym. J.* **22**(5) (1990) 355
20. Swedish Transmission Research Institute, "Hydrophobicity Classification Guide", Guide 1, 92/1 (1992)
21. F. W. SHEN, H. A. MCKELLOP and R. SALOVEY, *J. Polym. Sci. Part B, Polym. Phys.* **34** (1996) 1063
22. M. H. NAKA, Y. MORITA and K. IKEUCHI, *Proc. Inst. Mech. Eng. [H]* **219**(3) (2005) 175
23. U. RAVIV, J. FREY, R. SAK, P. LAURAT, R. TADMOR and J. KLEIN, *Langmuir* **18** (2002) 7482
24. S. P. HO, N. NAKABAYASHI, Y. IWASAKI, T. BOLAND and M. LABERGE, *Biomaterials* **24** (2003) 5121
25. K. ISHIHARA, D. NISHIUCHI, J. WATANABE and Y. IWASAKI, *Biomaterials* **25** (2004) 1115
26. O. K. MURATOGLU, C. R. BRAGDON, D. O. O'CONNOR, M. JASTY, W. H. HARRIS, R. GUL and F. MCGARRY, *Biomaterials* **20** (1999) 1463

Enhanced wear resistance of modified cross-linked polyethylene by grafting with poly(2-methacryloyloxyethyl phosphorylcholine)

Masayuki Kyomoto,[1] Toru Moro,[2] Tomohiro Konno,[3] Hiroaki Takadama,[4] Noboru Yamawaki,[1] Hiroshi Kawaguchi,[2] Yoshio Takatori,[2] Kozo Nakamura,[2] Kazuhiko Ishihara[3]

[1]*Research and Development Corporate Division, Japan Medical Materials Corporation, Osaka, Japan*
[2]*Department of Orthopaedic Surgery, School of Medicine, The University of Tokyo, Tokyo, Japan*
[3]*Department of Materials Engineering, School of Engineering and Center for NanoBio Integration, The University of Tokyo, Tokyo, Japan*
[4]*Materials Research and Development Laboratory, Japan Fine Ceramics Center, Nagoya, Japan*

Received 17 May 2006; revised 28 September 2006; accepted 28 September 2006
Published online 30 January 2007 in Wiley InterScience (www.interscience.wiley.com). DOI: 10.1002/jbm.a.31134

Abstract: We developed a cross-linked polyethylene (CLPE) modified with a phospholipid polymer in order to address the serious problem of osteolysis caused by wear particles derived from the polyethylene components of artificial hip joints. Our goal of preventing aseptic loosening could be achieved by avoiding any formation of CLPE wear particles or suppressing the activation of cell systems by the wear particles. We investigated the surface and wear resistance properties of 2-methacryloyloxyethyl phosphorylcholine (MPC) polymer grafted onto the surface of CLPE (CLPE-*g*-MPC). The relative density of MPC polymer chains was determined by the P—O group index. Generally, polymerization times correspond to the number of polymer chains in radical polymerization. After 3.0 × 10^6 cycles in a hip joint simulator test, the steady wear rates of the untreated CLPE and CLPE-*g*-MPC cups with a low P—O group index were as high as 4 mg/10^6 cycles; those of the CLPE-*g*-MPC cups with high P—O group indexes, that is, 0.46 and 0.48, markedly decreased to −1.12 and 0.16 mg/10^6 cycles, respectively. Therefore, the grafting of an MPC polymer with high density would be essential in order to maintain the long-term wear resistance of CLPE-*g*-MPC as an orthopedic bearing material. © 2007 Wiley Periodicals, Inc. J Biomed Mater Res 82A: 10–17, 2007

Key words: joint replacements; polyethylene; phospholipid; phosphorylcholine; wear mechanisms

INTRODUCTION

As the number of aged persons in the world increases year by year, the increase in patients with poorly functioning joints due to external injury or disease is becoming a serious social problem. This means that the quality of artificial joints is becoming increasingly important. Most patients who receive an artificial joint experience a dramatic relief of pain and enjoy a rapid improvement in the quality of life. The most widely used bearing couple for artificial joint systems is the combination of an ultra-high molecular weight polyethylene (UHMWPE) acetabular component and a metal (generally Co-Cr-Mo alloy) femoral component. However, osteolysis caused by wear particles of the UHMWPE is a serious problem with artificial hip joints.[1–3] Reducing wear particle production from UHMWPE is one way of preventing osteolysis. Efforts to decrease these particles have focused on using combinations other than metal-on-UHMWPE and improving the bearing materials themselves.

Several highly cross-linked polyethylenes (CLPE), irradiated with 50–105 kGy, have been launched since 1998 and used extensively.[4,5] Gamma and electron beam irradiation at various doses are used to produce CLPE and numerous *in vitro* studies have been performed using it. In published studies, CLPE subjected to 50–105 kGy exhibited an 80–90% reduc-

Correspondence to: M. Kyomoto, Japan Medical Materials Corporation, Uemura Nissei Bldg. 9F 3-3-31 Miyahara, Yodogawa-Ku, Osaka 532-0003, Japan; e-mail: kyomotom@jmmc.jp

Contract grant sponsor: Japanese Ministry of Education, Culture, Sports, Science, and Technology; contract grant number: 15390449
Contract grant sponsor: Japanese Ministry of Health, Labor, and Welfare

tion in wear rate compared with conventional polyethylene.[6,7] Furthermore, clinical results have confirmed CLPE's effective wear-resistance. However, while the efficacy of the CLPE is evidenced by these reports, *in vivo* the reduction of wear is reported to be only 40–60%.[8–12] Therefore, further improvement of CLPE is desirable.

Recently, we have developed a new-concept artificial hip joint with 2-methacryloyloxyethyl phosphorylcholine (MPC) polymer grafted onto the surface of CLPE (CLPE-*g*-MPC); it has been designed to reduce wear and suppress bone resorption.[13] MPC, a methacrylate monomer with a phospholipid polar group in the side chain, is a novel biomaterial designed and developed by Ishihara et al. that mimics the neutral phospholipids of biomembranes.[14] Various polymers containing MPC units are already widely used as biomaterials.[15,16] The biomembrane-like surface is readily obtained by treating the substrate materials with MPC polymer. The artificial biomembrane surface thus formed exhibits excellent biocompatibility; it is hydrophilic and forms a thin film of free water under physiological conditions.[17] Several medical devices have already been developed utilizing MPC polymer. These devices have been subjected to clinical use with the approval of the Food and Drug Administration of the USA; therefore, the efficacy and safety of the MPC polymer as a biomaterial are well established.[18–20]

We have been developing novel artificial joints with very-low-friction bearing surfaces by combining the biocompatible and hydrophilic MPC polymer with CLPE; this has been accomplished by using a photo-induced radical polymerization technique. This technique facilitates direct grafting of MPC to CLPE, thereby forming C—C covalent bonding between the MPC polymer and CLPE substrate. The advantage of this technique is that the MPC polymer graft occurs only on the CLPE surface and has no effect on the bulk properties of the CLPE substrate. The present study investigated the structure and properties of the MPC polymer layer formed on the CLPE surface by photo-induced radical graft polymerization. The wear-resistant properties of the CLPE-*g*-MPC are discussed in terms of the characteristics of the MPC polymer layer.

MATERIALS AND METHODS

Chemicals

Benzophenone and acetone were purchased from Wako Pure Chemical Industries (Osaka, Japan). 2-Methacryloyloxyethyl phosphorylcholine (MPC) was synthesized industrially using the method reported by Ishihara et al.[14] and was supplied by Ai Bio-Chips Co. (Tokyo, Japan).

MPC graft polymerization

Compression-molded UHMWPE (GUR1020 resin; Poly Hi Solidur, IN) bar stock was γ-irradiated with 50 kGy in N_2 gas and annealed at 120°C for 7.5 h in N_2 gas for cross-linking. The cross-linked polyethylene (CLPE) specimens were machined from this bar stock after cooling. The specimens were immersed in an acetone solution containing 10 mg/mL benzophenone for 30 s and then dried in the dark to remove acetone at room temperature. The amount of benzophenone adsorbed on the surface was determined by ultraviolet spectroscopy to be 3.5×10^{-11} mol/cm^2 using a previously described method.[21] The MPC monomer was dissolved in degassed pure water to a concentration of 0.5 mol/L. The CLPE specimens coated with benzophenone were immersed in the aqueous MPC solution. The photo-induced graft polymerization on the CLPE surface was carried out with ultraviolet irradiation of 5 mW/cm^2 for 10–360 min at 60°C using a Toshiba D-35 filter that permitted the passage of ultraviolet light with a wavelength of 350 ± 50 nm only. After the polymerization, the CLPE-*g*-MPC specimens were removed, washed with pure water and ethanol, and then dried. The CLPE-*g*-MPC specimens were gamma-sterilized with a dose of 25 kGy under N_2 gas.

Surface analysis by using XPS, water-contact angle measurement, and FT-IR/ATR

The surface elemental conditions of the CLPE before and after MPC grafting were analyzed by X-ray photoelectron spectroscopy (XPS). The XPS spectra were obtained using an AXIS-HSi165 spectrophotometer (Kratos Analytical, UK) equipped with an Mg-Kα radiation source at 15 kV at the anode. The take-off angle of the photoelectrons was maintained at 90°. Five scans were taken for each sample.

The static water-contact angle of the CLPE-*g*-MPC with various photo-polymerization periods was measured by a sessile drop method using an optical bench-type contact angle goniometer (Model DM300; Kyowa Interface Science Co., Saitama, Japan). Drops of purified water (1 μL) were deposited onto the surface of the CLPE-*g*-MPC and the contact angles were directly measured with a microscope after each dropping (60 s), according to the ISO 15989 standard.[22] Fifteen replicate measurements were performed on each sample and the contact angle values were averaged.

The functional-group vibrations of the CLPE-*g*-MPC surface with various photo-polymerization periods were examined by Fourier-transform infrared (FT-IR) spectroscopy with attenuated total reflection (ATR) equipment. The measurements were performed over a range of 800–2000 cm^{-1} by using an FT-IR analyzer (Perkin-Elmer FT-IR 1650; Perkin-Elmer Corp., MA) at a resolution of 4.0 cm^{-1} for 100 scans.

The relative amount of grafted MPC polymer unit on the CLPE surface was evaluated by quantification of the phosphate (P—O) group that is contained within the structure of the MPC unit. The relative amount of phosphate

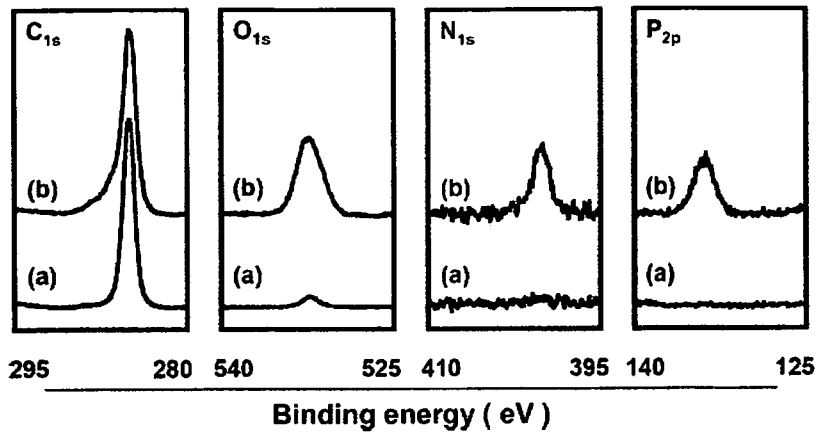

Figure 1. XPS spectra of CLPE-*g*-MPC. (a) CLPE (untreated), (b) CLPE-*g*-MPC.

group was defined as the P—O group index and was calculated as follows.

$$\text{P—O group index} = (1080\ \text{cm}^{-1}\ \text{peak intensity})/(1460\ \text{cm}^{-1}\ \text{peak intensity})$$

Cross-section of CLPE-*g*-MPC observed with TEM

A cross-section of the MPC polymer layer on the CLPE-*g*-MPC surface produced by various photo-polymerization periods was observed with a transmission electron microscope (TEM). The specimens (two pieces for each irradiation time) were first embedded in epoxy resin, stained with ruthenium oxide vapor at room temperature, and then sliced into ultra-thin films (~100-nm thick) by using a Leica Ultra Cut UC microtome (Leica Microsystems, Wetzlar, Germany). A JEM-1010 electron microscope (JEOL, Tokyo, Japan) was used for the TEM observation at an acceleration voltage of 100 kV.

Hip simulation wear test

The inner and outer diameters of the CLPE-*g*-MPC cups used in the hip joint simulator were 26 mm and 52 mm, respectively. For each irradiation time (0, 23, 45, 90, and 180 min) four pieces were prepared. The wear test was performed using a 12-station hip joint simulator (MTS system Corp., MN). A 26-mm Co-Cr-Mo alloy femoral ball component (Japan Medical Materials Corp., Osaka, Japan) was used as an acetabular component. A mixture of 25% bovine serum, 20 m*M*/L of ethylenediaminetetraacetic acid (EDTA), and 0.1% sodium azide was used as lubricant, according to the ISO 14242-1 standard.[23] The lubricant was replaced every 0.5×10^6 cycles. Walks, simulating a physiologic loading curve (Paul-type) with double peaks of 1793 and 2744*N* (183 and 280 kgf) loads, were applied with multidirectional (biaxial and orbital) motion of 1 Hz frequency. The wear was determined by weighing the polyethylene cups. Load-soak controls ($n = 2$) were used to compensate for fluid absorption by the wear specimens.[24] The weights of the cups were measured every 0.5×10^6 cycles. The testing continued until a total of 3.5×10^6 cycles were completed.

To evaluate the net wear, corrected for any influence from plastic deformation, a melt-recovery operation was performed on selected samples of both CLPE and CLPE-*g*-MPC cups after the simulator tests, according to the method of Muratoglu et al.[25] The cups were melted at 150°C in a vacuum and allowed to cool down to the room temperature. The surface features of the bearing surfaces of the cups were observed with a confocal laser scanning microscope (OLS1200; Olympus Corp., Tokyo, Japan).

RESULTS

Figure 1 shows the XPS spectra (C_{1s}, O_{1s}, N_{1s}, and P_{2p}) of CLPE and CLPE-*g*-MPC. In the C_{1s} spectra of both CLPE and CLPE-*g*-MPC a strong peak was observed at 285 eV. This peak is attributed to the carbon atoms in the C—C or C—H groups. In the O_{1s} spectrum of CLPE-*g*-MPC, a significant peak assigned to the C—O group was observed at 532 eV. This peak is mainly ascribed to the MPC units. Even untreated CLPE exhibited a small peak at 532 eV. In this case, the peak is attributed to oxygen atoms and might suggest the contamination and/or oxidation of the CLPE surface. In the N_{1s} and P_{2p} spectra, clear peaks were observed for CLPE-*g*-MPC only. Peaks at 403 and 134 eV were assigned to the $-N^+(CH_3)_3$ and phosphate groups, respectively; these peaks are characteristic of the phosphorylcholine in the MPC units. Table I summarizes the elemental compositions of the surfaces of untreated CLPE and CLPE-*g*-MPC. The measured contents of nitrogen (*N*) and phosphorous (*P*) in the CLPE-*g*-MPC was 5.1 and 5.2, respectively. These values were almost equivalent to the theoretical values ($N = 5.3$, $P = 5.3$) of MPC polymer.

Figure 2 shows the FT-IR/ATR spectra of CLPE and CLPE-*g*-MPC. A transmittance absorption peak was observed at 1460 cm^{-1} for both CLPE and

TABLE I
Surface Elemental Compositions (%) of CLPE (Untreated) and CLPE-g-MPC

Samples	C	O	N	P
Untreated CLPE	99.6 (100.0)	0.4 (0.0)	0.0 (0.0)	0.0 (0.0)
CLPE-g-MPC	61.8 (57.9)	27.9 (31.6)	5.1 (5.3)	5.2 (5.3)

Theoretical elemental compositions of CLPE and MPC polymer are shown in the parentheses, respectively.

CLPE-g-MPC. This peak is attributed mainly to the methylene (CH_2) chain in the CLPE substrate since the peak intensity is very strong and it is unchanged between the CLPE and the CLPE-g-MPC. However, the transmittance absorption peaks at 1240, 1080, and 970 cm^{-1} were observed only for the CLPE-g-MPC. These peaks are ascribed to the phosphate (P—O) group in the MPC unit. Similarly, the transmittance absorption peak at 1720 cm^{-1} observed for CLPE-g-MPC only corresponds to the ketone group in the MPC unit.

The relative P—O group index was calculated from the ratio of the FT-IR peak intensities at 1080 and 1460 cm^{-1} as a measure of the amount of MPC unit grafted onto the CLPE surface; this was done because the peak intensity at 1460 cm^{-1} remains unchanged.

Figure 3 shows the calculated P—O group index as a function of the irradiation time for the CLPE-g-MPC specimens. The P—O group index increased as the irradiation time was increased.

Figure 4 shows the static water-contact angle as a function of the calculated P—O group index for the CLPE-g-MPC specimens. The static water-contact angle on the untreated CLPE was 88° and decreased markedly with an increase in the P—O group index. When the P—O group index was greater than 0.3, the static water-contact angle became constant at the low value of 15°.

Figure 5 shows cross-sectional TEM images of CLPE-g-MPC produced with various ultraviolet irradiation times during polymerization. Lamellae of the order of 100–400 nm in length and 10–20 nm in thickness were observed in the CLPE substrate regardless of irradiation time, and the lamellae were 50–100 nm in length and 5–15 nm in thickness near the surface. With irradiation times longer than

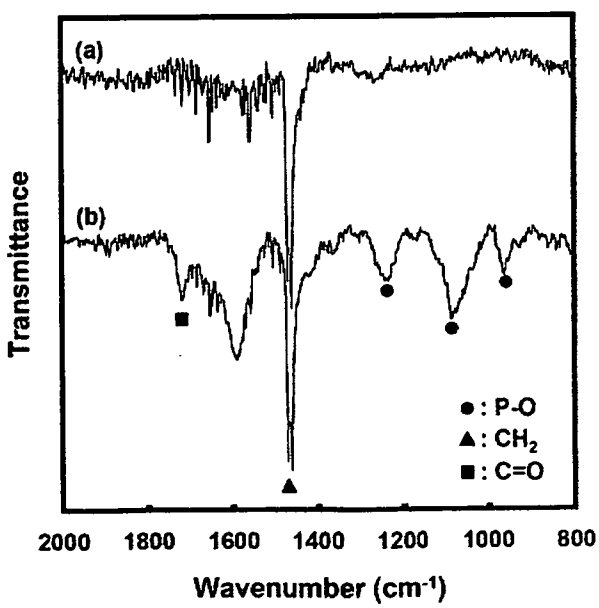

Figure 2. FT-IR/ATR spectra of CLPE-g-MPC. (a) CLPE (untreated), (b) CLPE-g-MPC.

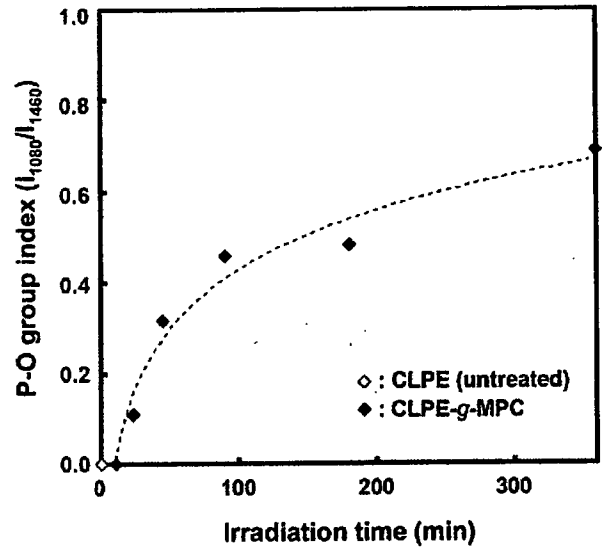

Figure 3. P—O group index as a function of irradiation time for CLPE-g-MPC.

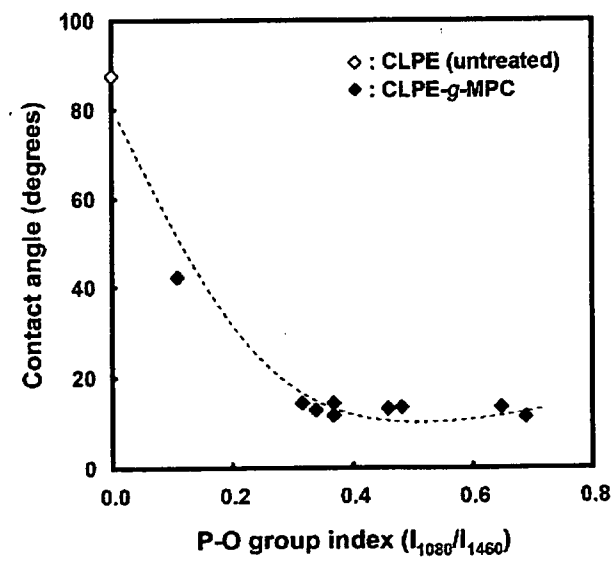

Figure 4. Static water-contact angle as a function of P—O group index for CLPE-g-MPC.

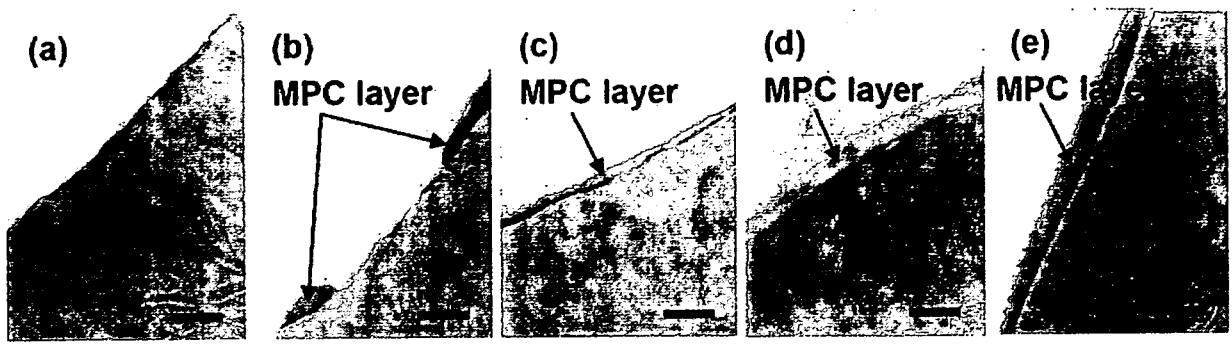

Figure 5. Cross-section TEM images of CLPE-*g*-MPC with various photo-polymerization times. Bar = 200 nm. (a) 11 min, (b) 23 min, (c) 45 min, (d) 90 min, and (e) 180 min.

45 min, a grafted MPC polymer layer 100–200 nm thick was clearly observed on the surface of the CLPE substrate. The MPC-covered region was coexistent with uncovered regions after an irradiation time of 23 min, although the thickness on the MPC polymer layer of the covered region remained the same (100–200 nm). With irradiation for 11 min, no MPC graft layer was observed on the surface of the CLPE. These results indicate that the density of the grafted MPC polymer can be controlled by the polymerization time. This is attributable to the fact that the number of polymer chains produced in a radical polymerization reaction is generally correlated with the photo-irradiation time.

Figure 6 shows the gravimetric wear of CLPE-*g*-MPC with various polymerization irradiation times during the hip joint simulation test. The CLPE-*g*-MPC cups were found to wear significantly less than the untreated CLPE cups. The wear of the CLPE-*g*-MPC cups subjected to 23 min of irradiation started to increase after 2.5×10^6 cycles. Table II shows the wear rate of the CLPE-*g*-MPC cups with various P—O group indexes and irradiation times during the hip joint simulation test. We defined the initial wear rate as that from the start to 0.5×10^6 cycles, and considered the steady wear rate as that from 2.5×10^6 to 3.0×10^6 cycles. All of the untreated CLPE and CLPE-*g*-MPC cups showed low initial wear rates of −1.42 to −3.74 mg/10^6 cycles. The steady wear rate of the untreated CLPE cups and the CLPE-*g*-MPC cups with a low P—O group index of 0.11 increased to 3.68 and 4.64 mg/10^6 cycles, respectively. In contrast, the wear rates of the CLPE-*g*-MPC cups with high P—O group indexes, that is, 0.46 and 0.48, were markedly lower at −1.12 and 0.16 mg/10^6 cycles, respectively.

Figure 7 shows the confocal laser scanning microscopy images of the bearing surfaces of the untreated CLPE and CLPE-*g*-MPC (irradiation time = 90 min) cups before and after the melt-recovery test that was preformed after the simulator test. Before melt-recovery test, scratches were seen in the bearing surfaces of the untreated CLPE and CLPE-*g*-MPC. After melt-recovery test, these scratches completely disappeared from the bearing surfaces. In addition, clear regular circular machining marks were observed on the surface of the CLPE-*g*-MPC, while no marks were observed on the untreated CLPE, indicating that the former was not significantly worn.

DISCUSSION

We have developed an artificial hip joint that uses CLPE-*g*-MPC on the bearing surface; it has been designed to reduce wear and suppress bone resorption. Our previous study reported the effects of graft polymerization of MPC onto the CLPE surface.[13] The MPC grafting markedly decreased the friction and amount of wear. In the present study, we investigated the structure and properties of the MPC polymer layer formed on the CLPE surface by photo-induced

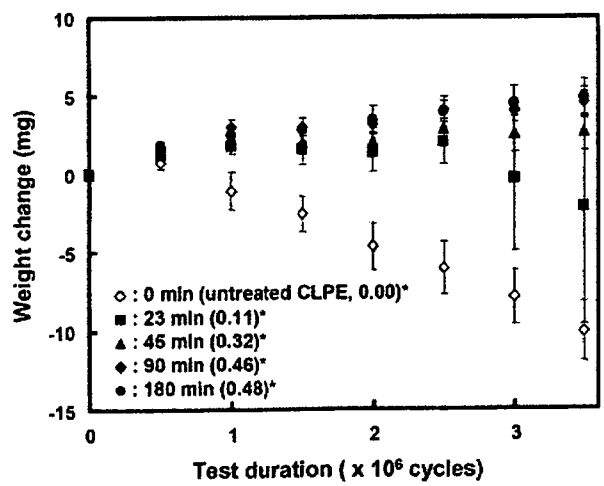

Figure 6. Weight change of CLPE-*g*-MPC cups with various irradiation times during polymerization in the hip joint simulation test. Bars = standard deviations. *P—O group indexes are in parentheses.

TABLE II
Typical P-O Group Index and Wear Rate in Hip Joint Simulator Tests

Irradiation Time (min)	P—O Group Index (I_{1080}/I_{1460})	Initial Wear Rate (mg/10^6 cycles)	Steady Wear Rate (mg/10^6 cycles)
0 (untreated CLPE)	0.00	−1.42 (0.78)	3.68 (0.20)
23	0.11	−2.78 (0.76)	4.64 (6.38)
45	0.32	−2.58 (0.08)	0.68 (0.80)
90	0.46	−3.60 (0.48)	−1.12 (0.32)
180	0.48	−3.74 (0.50)	0.16 (0.08)

The standard deviation is in parentheses.

radical graft polymerization; this report discusses the wear-resistant properties of CLPE-g-MPC in terms of the characteristics of the MPC polymer layer.

After 3.0 × 10^6 cycles of the hip joint simulator test, we confirmed that the CLPE-g-MPC cups with a P—O group index of 0.32 to 0.48 exhibited a relatively low steady wear rate (−1.12 to 0.68 mg/10^6 cycles). This indicates that CLPE-g-MPC cups with a P—O group index greater than 0.32 achieve a >80% reduction in their steady wear rate compared with untreated CLPE as well as CLPE-g-MPC cups with a low P—O group index (0.11) and low density of grafted MPC polymer chains. Since MPC is a highly hydrophilic compound, poly(MPC) is water-soluble. In fact, as shown in Figure 4, the water-wettability of the CLPE-g-MPC surface was considerable greater than that of an untreated CLPE surface. Therefore, the artificial hip joint bearing with the grafted MPC polymer surface exhibited considerably higher lubricity than that without the MPC polymer. The significant reduction in the coefficient of friction of the grafted MPC polymer[13] resulted in a substantial improvement in wear resistance. We assumed that the bearing surface of the artificial hip joint combined with MPC polymer exhibited the fluid film lubrication (or mixed lubrication) of the intermediate hydrated layer; this suggests that this novel artificial hip joint mimics the natural joint cartilage.

It is assumed that several important issues are involved in the long-term retention of the benefits of MPC polymer used in artificial joints under variable and multidirectional loads: strong bonding between the MPC polymer and the CLPE surface, high mobility of the free end groups of the MPC polymer, and a high density of the introduced MPC polymer. These considerations are based on previous studies

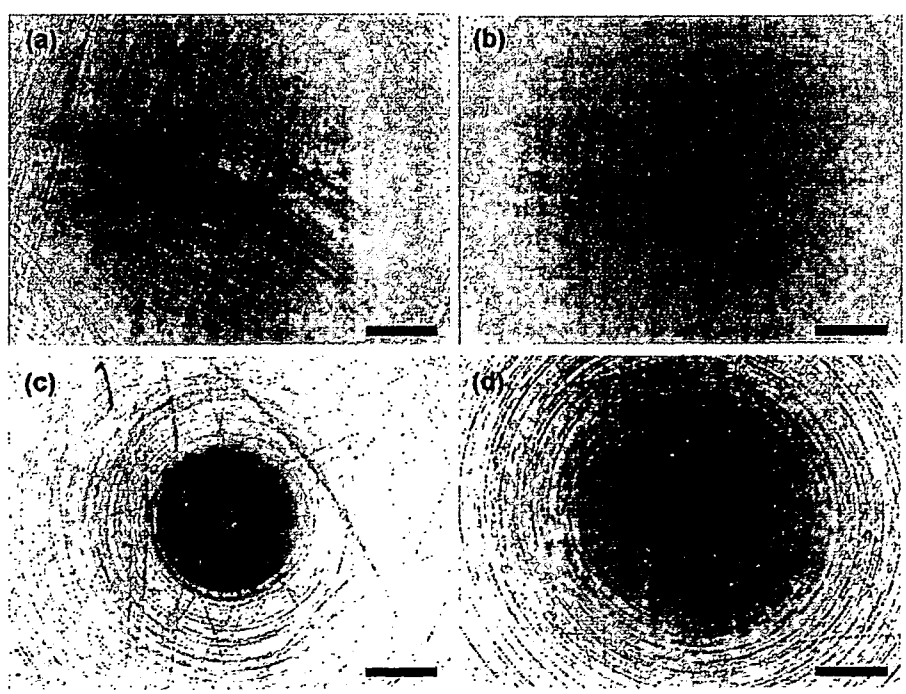

Figure 7. Confocal laser scanning microscope images of the bearing surfaces of the cups before and after a melt-recovery test that was performed after the simulator test. (a) CLPE before melt-recovery test, (b) CLPE after melt-recovery test, (c) CLPE-g-MPC before melt-recovery test, and (d) CLPE-g-MPC after melt-recovery test. Bar = 400 μm.

of charged polymers (polyelectrolytes) reported by Raviv et al.[26,27] With this in mind, we selected photo-induced radical graft polymerization to produce C—C covalent bonding between a carbon atom of CLPE and an end group of the MPC polymer chain. As shown in Figure 5, the crystalline structure of the CLPE substrate is unchanged even after the grafting of MPC, regardless of irradiation time (polymerization time). This indicates that ultraviolet-induced radical graft polymerization does not affect the structure of the CLPE substrate. The unchanged structure of the CLPE substrate itself is very important because the CLPE cup acts not only as a bearing material but also as a structural material in the artificial hip joint. Furthermore, when the MPC layer disappears on the substrate surface, the exposed CLPE substrate may have lower wear than uncross-linked polyethylenes. We therefore deemed that the substrate was CLPE, although it was shielded by the MPC layer. In a previous study using gamma irradiation,[28] the lower-molecular-weight cross-linked GUR1020 materials had higher mechanical properties (tensile and impact properties) for all doses compared to the higher-molecular-weight cross-linked GUR1050 materials. Nevertheless, the cross-linked GUR1020 materials exhibited the same wear rate as the cross-linked GUR1050 materials. Therefore, we selected the GUR1020 compression-molded bar stock as a CLPE substrate.

To obtain an MPC polymer layer with high density, the irradiation time must be controlled.[20] The density of the MPC polymer chains on the surface of the CLPE gradually increased with increasing irradiation time and the entire surface of the CLPE was coated using polymerization times longer than 45 min. As shown in Figure 5, with longer irradiation, the thickness of the MPC polymer layer remained the same (100–200 nm). In the CLPE-*g*-MPC cups with a high surface density of MPC graft chains, the MPC graft chains are assumed to stand up to exhibit a brush like structure.[29,30] It is generally well-known that the reaction rate of radical polymerization is extremely high.[31] The molecular weight of grafted polymer is therefore controlled by monomer concentration. When the MPC polymer layer has brush like structure, the layer thickness might depend on the molecular weight of grafted MPC polymer. On the other hand, Figure 4 implies that the density of the MPC polymer chains on the surface of the CLPE was different, even if the water-wettability of the CLPE-*g*-MPC was constant (as low as 15°); this is because the P—O group index changed remarkably within the range of 0.3 and 0.7.

As mentioned above, the steady wear rate of CLPE-*g*-MPC cups with a high P—O group index was relatively low even after 3.5×10^6 cycles in the simulator test. As shown in Figure 7, clear machining marks with regular circles remained on the surface of CLPE-*g*-MPC cups even after the simulator test. In other words, the CLPE-*g*-MPC cups were virtually unworn, which is consistent with the relatively low wear observed in the hip joint simulator tests.

Table II shows that several CLPE-*g*-MPC cups exhibited a slight increase in weight (wear rate was negative); this was attributable to slightly enhanced fluid absorption over and above the fluid absorption by the load-soak controls. When using the gravimetric method, we corrected the weight loss for the fluid absorption by subtracting the weight gain that occurred in the load-soak controls. Since the wear cups are subjected to motion and load, there are limitations to this correction; therefore, they are observed to absorb slightly more fluid than their load-soak controls. However, as a result, the correction for fluid absorption by using the load-soak controls data as the correction factor leads to a slight underestimation of the actual weight loss.

The excellent functions of CLPE-*g*-MPC could avoid the activation of cell systems by the wear particles, thus entirely preventing periprosthetic osteolysis and subsequent aseptic loosening.[13] In view of its superior mechanical and biological advantages, the CLPE-*g*-MPC is widely expected to be the next-generation bearing material for artificial hip joints. Arrangements are now being made for the conduction of clinical trials.

In this study, we investigated the surface physical properties of CLPE-*g*-MPC. After a hip joint simulator test, we confirmed that CLPE-*g*-MPC cups with a high surface density of MPC graft chains exhibited a relatively low and steady wear rate. When compared with cups with untreated CLPE and those with CLPE-*g*-MPC with a low P—O group index (cups with low density of grafted MPC polymer chain), these CLPE-*g*-MPC cups exhibited an 80% reduction in their steady wear rate. Thus, it appears that CLPE-*g*-MPC markedly reduces the generation of wear particles. However, the grafting of MPC polymer at a high density is essential to maintain the wear-resistance of CLPE-*g*-MPC as an orthopedic bearing material over long periods of time. We conclude that grafting MPC onto CLPE is a useful method for maintaining efficient lubrication of artificial hip joints over a long period.

The authors thank Dr. Fumiaki Miyaji, Mr. Yoshiki Ando, and Mr. Takatoshi Miyashita (Japan Medical Materials Corp., Osaka, Japan) for their excellent technical assistance.

References

1. Harris WH. The problem is osteolysis. Clin Orthop 1995;311:46–53.

2. Kobayashi A, Freeman MA, Bonfield W, Kadoya Y, Yamac T, Al-Saffar N, Scott G, Revell PA. Number of polyethylene particles and osteolysis in total joint replacements. A quantitative study using a tissue-digestion method. J Bone Joint Surg Br 1997; 79:844–848.
3. Sochart DH. Relationship of acetabular wear to osteolysis and loosening in total hip arthroplasty. Clin Orthop 1999;363: 135–150.
4. Collier JP, Currier BH, Kennedy FE, Currier JH, Timmins GS, Jackson SK, Brewer RL. Comparison of cross-linked polyethylene materials for orthopaedic applications. Clin Orthop Relat Res 2003;414:299–304.
5. Muratoglu OK, Mark A, Vittetoe DA, Harris WH, Rubash HE. Polyethylene damage in total knees and use of highly crosslinked polyethylene. J Bone Joint Surg Am 2003;85:S7–S13.
6. McKellop H, Shen FW, Lu B, Campbell P, Salovey R. Development of an extremely wear-resistant ultra high molecular weight polyethylene for total hip replacements. J Orthop Res 1999;17:157–167.
7. Muratoglu OK, Bragdon CR, O'Connor DO, Jasty M, Harris WH. A novel method of crosslinking ultra-high-molecular-weight polyethylene to improve wear, reduce oxidation, and retain mechanical properties. Recipient of the 1999 HAP Paul Award. J Arthroplasty 2001;16:149–160.
8. Manning DW, Chiang PP, Martell JM, Galante JO, Harris WH. In vivo comparative wear study of traditional and highly cross-linked polyethylene in total hip arthroplasty. J Arthroplasty 2005;20:880–886.
9. Digas G, Kärrholm J, Thanner J, Malchau H, Herberts P. Highly cross-linked polyethylene in cemented THA. Clin Orthop Relat Res 2003;417:126–138.
10. Heicel C, Silva M, dela Rosa MA, Schmalzried TP. Short-term in vivo wear of cross-linked polyethylene. J Bone Joint Surg Am 2004;86:748–751.
11. Martell JM, Verner JJ, Incavo SJ. Clinical performance of a highly cross-linked polyethylene at two years in total hip arthroplasty: A randomized prospective trial. J Arthroplasty 2003;18:55–59.
12. Oonishi H, Kim SC, Takao Y, Kyomoto M, Iwamoto M, Ueno M. Wear of highly cross-linked polyethylene acetabular cup in Japan. J Arthroplasty 2006;18:944–949.
13. Moro T, Takatori Y, Ishihara K, Konno T, Takigawa Y, Matsushita T, Chung UI, Nakamura K, Kawaguchi H. Surface grafting of artificial joints with a biocompatible polymer for preventing periprosthetic osteolysis. Nat Mater 2004;3:829–837.
14. Ishihara K, Ueda T, Nakabayashi N. Preparation of phospholipid polymers and their properties as polymer hydrogel membranes. Polym J 1990;22:355–360.
15. Ishihara K, Aragaki R, Ueda T, Watanabe A, Nakabayashi N. Reduced thrombogenicity of polymers having phospholipid polar groups. J Biomed Mater Res 1990;24:1069–1077.
16. Ishihara K, Ziats NP, Tierney BP, Nakabayashi N, Anderson JM. Protein adsorption from human plasma is reduced on phospholipids polymers. J Biomed Mater Res 1991;25:1397–1407.
17. Kitano H, Imai M, Mori T, Gemmei-Ide M, Yokoyama Y, Ishihara K. Structure of water in the vicinity of phospholipid analogue copolymers as studied by vibrational spectroscopy. Langmuir 2003;19:10260–10266.
18. Kuiper KJ, Nordrehaug JE. Early mobilization after protamine reversal of heparin following implantation of phosphorylcholine-coated stents in totally occluded coronary arteries. Am J Cardiol 2000;85:698–702.
19. Galli M, Sommariva L, Prati P, Zerboni S, Politi A, Bonatti R, Mameli S, Butti E, Pagano A, Ferrari G. Acute and mid-term results of phosphorylcholine-coated stents in primary coronary stenting for acute myocardial infarction. Catheter Cardiovasc Interv 2001;53:182–187.
20. Lewis AL, Tolhurst LA, Stratford PW. Analysis of a phosphorylcholine-based polymer coating on a coronary stent pre- and post-implantation. Biomaterials 2002;23:1697–1706.
21. Ishihara K, Iwasaki Y, Ebihara S, Shindo Y, Nakabayashi N. Photoinduced graft polymerization of 2-methacryloyloxyethyl phosphorylcholine on polyethylene membrane surface for obtaining blood cell adhesion resistance. Colloids Surf B 2000; 18:325–335.
22. ISO. Plastics—Film and sheeting—Measurement of water-contact angle of corona-treated films. 2004. International Organization for Standardization 15989.
23. ISO. Implants for surgery: Wear of total hip-joint prostheses, Part 1: Loading and displacement parameters for wear-testing machines and corresponding environmental conditions for test. 2002. International Organization for Standardization 14242-1.
24. ISO. Implants for surgery: Wear of total hip-joint prostheses, Part 2: Methods of measurement. 2000. International Organization for Standardization 14242-2.
25. Muratoglu OK, Greenbaum ES, Bragdon CR, Jasty M, Freiberg AA, Harris WH. Surface analysis of early retrieved acetabular polyethylene liners: A comparison of conventional and highly crosslinked polyethylenes. J Arthroplasty 2004;19: 68–77.
26. Raviv U, Frey J, Sak R, Laurat P, Tadmor R, Klein J. Properties and interactions of physigrafted end-functionalized poly (ethylene glycol) layers. Langmuir 2002;18:7482–7495.
27. Raviv U, Glasson S, Kampf N, Gohy JF, Jérôme R, Klein J. Lubrication by charged polymers. Nature 2003;425:163–165.
28. Greer KW, King RS, Chan FW. The effects of raw material, irradiation dose, and irradiation source on crosslinking of UHMWPE. In: Kurtz SM, Gsell RA, Martell J, editors. Crosslinked and Thermally Treated Ultra-High Molecular Weight Polyethylene for Joint Replacements. West Conshohoken: American Society for Testing and Materials; 2003. pp 209–220.
29. Matsuda T, Kaneko M, Ge S. Quasi-living surface graft polymerization with phosphorylcholine group(s) at the terminal end. Biomaterials 2003;24:4507–4515.
30. Goda T, Konno T, Takai M, Moro T, Ishihara K. Biomimetic phosphorylcholine polymer grafting from polydimethylsiloxane surface using photo-induced polymerization. Biomaterials 2006;27:5151–5160.
31. Feng W, Brash J, Zhu S. Atom-transfer radical grafting polymerization of 2-methacryloyloxyethyl phosphorylcholine from silicon wafer surface. J Polym Sci Part A: Polym Chem 2004;42: 2931–2942.

Available online at www.sciencedirect.com
ScienceDirect
Colloids and Surfaces B: Biointerfaces 57 (2007) 226–236
COLLOIDS AND SURFACES B
www.elsevier.com/locate/colsurfb

Surface modification with well-defined biocompatible triblock copolymers
Improvement of biointerfacial phenomena on a poly(dimethylsiloxane) surface

Yasuhiko Iwasaki [a,*], Mika Takamiya [a,c], Ryoko Iwata [a], Shin-ichi Yusa [d], Kazunari Akiyoshi [a,b]

[a] *Institute of Biomaterials and Bioengineering, Tokyo Medical and Dental University, 2-3-10 Kanda-surugadai, Chiyoda-ku, Tokyo 101-0062, Japan*
[b] *Center of Excellence Program for Frontier Research on Molecular Destruction and Reconstruction of Tooth and Bone, Tokyo Medical and Dental University, 2-3-10 Kanda-surugadai, Chiyoda-ku, Tokyo 101-0062, Japan*
[c] *Department of Chemistry, Faculty of Science, Toho University, 2-2-1 Miyama, Funabashi-shi, Chiba 274-8510, Japan*
[d] *Department of Materials Science and Chemistry, Graduate School of Engineering, University of Hyogo, 2167 Shosha, Himeji-shi, Hyogo 671-2280, Japan*

Received 12 November 2006; received in revised form 8 January 2007; accepted 3 February 2007
Available online 11 February 2007

Abstract

To improve interfacial phenomena of poly(dimethylsiloxane) (PDMS) as biomaterials, well-defined triblock copolymers were prepared as coating materials by reversible addition-fragmentation chain transfer (RAFT) controlled polymerization. Hydroxy-terminated poly(vinylmethylsiloxane-co-dimethylsiloxane) (HO–PV_lD_mMS–OH) was synthesized by ring-opening polymerization. The copolymerization ratio of vinylmethylsiloxane to dimethylsiloxane was 1/9. The molecular weight of HO–PV_lD_mMS–OH ranged from (1.43 to 4.44) × 10^4, and their molecular weight distribution (M_w/M_n) as determined by size-exclusion chromatography equipped with multiangle laser light scattering (SEC-MALS) was 1.16. 4-Cyanopentanoic acid dithiobenzoate was reacted with HO–PV_lD_mMS–OH to obtain macromolecular chain transfer agents (macro-CTA). 2-Methacryloyloxyethyl phosphorylcholine (MPC) was polymerized with macro-CTAs. The gel-permeation chromatography (GPC) chart of synthesized polymers was a single peak and M_w/M_n was relatively narrow (1.3–1.6). Then the poly(MPC) (PMPC)–PV_lD_mMS–PMPC triblock copolymers were synthesized. The molecular weight of PMPC in a triblock copolymer was easily controllable by changing the polymerization time or the composition of the macro-CTA to a monomer in the feed. The synthesized block copolymers were slightly soluble in water and extremely soluble in ethanol and 2-propanol.

Surface modification was performed *via* hydrosilylation. The block copolymer was coated on the PDMS film whose surface was pretreated with poly(hydromethylsiloxane). The surface wettability and lubrication of the PDMS film were effectively improved by immobilization with the block copolymers. In addition, the number of adherent platelets from human platelet-rich plasma (PRP) was dramatically reduced by surface modification. Particularly, the triblock copolymer having a high composition ratio of MPC units to silicone units was effective in improving the surface properties of PDMS.

By selective decomposition of the Si–H bond at the surface of the PDMS substrate by irradiation with UV light, the coating region of the triblock copolymer was easily controlled, resulting in the fabrication of micropatterns. On the surface, albumin adsorption was well manipulated.

Keywords: Phosphorylcholine polymer; PDMS; RAFT polymerization; Block copolymer; Surface modification; Non-fouling; Lubrication

1. Introduction

Poly(dimethylsiloxane) (PDMS) is one of the most valuable polymers for use in biomedical devices such as catheters, tracheoesophageal voice prostheses, finger joints, percutaneous devices, dentures, etc. [1]. One of the more recent trends in PDMS applications is microfluidic devices for biosensors or

* Corresponding author. Tel.: +81 3 5280 8022; fax: +81 3 5280 8027.
E-mail address: yasu.org@tmd.ac.jp (Y. Iwasaki).

0927-7765/$ – see front matter © 2007 Elsevier B.V. All rights reserved.
doi:10.1016/j.colsurfb.2007.02.007

biochips [2–5]. PDMS has flexibility, high gas permeability, processability, flexible surface chemistry, and optical transparency. However, the interface of the PDMS surface with the biological environment is inadequate, and non-specific biofouling, i.e., protein adsorption and cell adhesion frequently occurs on the surface [6–9]. Biofouling induces contamination, inflammation, infection, and the reduction of material function. Highly friction of PDMS surface is also unfavorable nature for medical applications. These disadvantages of PDMS are due to hydrophobicity of the surface, necessitating surface modification. The formation of a hydrophilic surface on PDMS by using oxidization [10,11] and hydrophilic polymers [12–14] is proposed as a method of solving interfacial problems. Poly(ethylene glycol) (PEG) is one of the principal polymer candidates for reducing non-specific fouling at the biointerface [15]. For PDMS, covalent bonding onto PDMS surfaces of PEG-functionalized silanes [16–18] or amine-functionalized silanes to further react with PEG-moieties [19,20] has generally been employed. PEGylation is very effective in reducing biofouling. However, cell adhesion was observed on surfaces after long-term exposure in a culture medium [21].

To obtain other types of reliable non-fouling surfaces, we have been studying 2-methacryloyloxyethyl phosphorylcholine (MPC) polymers synthesized as biomimetics in biomembrane structures [22–24]. There have been some reports describing the surface modification of PDMS with MPC. Plasma-induced graft polymerization was applied as a primary process [25,26]. However, this modification has limitations in increasing the surface composition of MPC units because the phosphorus concentration remained low compared with the theoretical amount calculated from the chemical structure of MPC. Goda et al. recently reported the photo-induced grafting of MPC on a PDMS surface [14]. They succeeded in improving the composition of the MPC units on the PDMS surface compared with plasma polymerization. Moreover, the surface friction of PDMS surface effectively reduced by the surface modification. Although surface modification with MPC polymers *via* the grafting process is valuable for achieving a non-fouling surface on PDMS, their use precludes accurate control of the polymer structure and specific equipment is required.

Surface-coating processes are more applicable as methods of surface modification. Generally, organic solvent is used for the surface modification of PDMS, and the coating of hydrophilic polymer on PDMS is difficult because the surface is hydrophobic and has a low surface energy. The surface modification of PDMS using polar solvent is still limited [27]. A precise molecular design of an MPC polymer having the desired solubility and anchors that have an affinity to the PDMS surface is needed for reliable surface modification.

To produce well-defined polymers, controlled "living" radical polymerization has been explored [28]. Atom transfer radical polymerization (ATRP) and reversible addition-fragmentation chain transfer (RAFT) polymerization are very useful for achieving this process because they can be applied to a wide variety of monomers [29–35]. We have prepared poly(MPC) (PMPC) brush on a silicon wafer *via* ATRP and clarified that plasma protein adsorption and cell adhesion were effectively reduced on the surface with a polymer brush thickness of only 5 nm [36]. While the use of well-defined polymer brush with ATRP is considerable theoretical and experimental interests in control of surface properties, some specific conditions for the reaction are needed and still difficult to use as a common method of surface modification.

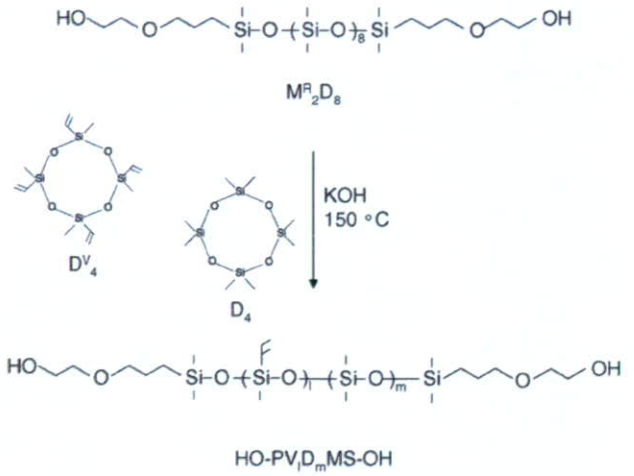

Scheme 1. Synthetic route of hydroxy-terminated poly(vinylmethylsiloxane-co-dimethylsiloxane) (OH–PV$_l$D$_m$MS–OH).

This paper primary reports surface modification of PDMS with well-defined ABA-type triblock copolymers composed of poly(MPC) (PMPC) blocks (A) and central silicone blocks (B) with anchoring vinyl groups by using a simple coating process. We also determine the effects of structures of the copolymers on the surface properties and clarify that the block copolymers have great power to improve interfacial phenomena of PDMS as biomaterials.

2. Materials and methods

2.1. Materials

Dicyclohexylcarbodiimide (DCC) and 4-dimethylaminopyridine was purchased from Kanto Chemical Co. Ltd., Japan and used without further purification. 4-Cyanopentanoic acid dithiobenzoate was synthesized according to the method reported by McCormick and co-workers [34]. Octamethylcyclotetrasiloxane (D_4), tetramethyl tetravinyl cyclotetrasiloxane (D^V_4), and hydroxyethoxypropyl dimethylsilyl-terminated oligo(dimethylsiloxane) ($M^R_2D_8$, $n=8$) were kindly provided by Shin-Etsu Chemical Co. Ltd. MPC was synthesized by the method previously described and purified by recrystallization from acetonitrile [23].

Hydroxy-terminated poly(vinylmethylsiloxane-co-dimethylsiloxane)s (HO–PV$_l$D$_m$MS–OH) were synthesized by conventional ring-opening polymerization of cyclosiloxane compounds using KOH (20 ppm) as a catalyst (Scheme 1). The molecular weight of hydroxy-terminated silicones was controlled by changing the ratio of D and $M^R_2D_8$. The ratio of D^V_4 and D_4 was adjusted at 1/9 in every case. The synthetic condition is summarized in Table 1. The absolute molecular weight (M_w)

Table 1
Synthetic results of hydroxy-terminated poly(dimethylsiloxane-co-vinylmethylsiloxane) (OH–PV_lD_mMS–OH)

Code	$M_2^RD_8/(Me_2SiO)_4/(MeViSiO)_4$ (mol)	Me_2SiO/MeViSiO (molar fraction)		M_w ($\times 10^4$)	M_w/M_n
		In feed	In copolymer[a]		
OH–$PV_{17}D_{173}$MS–OH	1/37/5	0.89/0.11	0.91/0.09	1.43[b]	1.16[b]
OH–$PV_{32}D_{324}$MS–OH	1/82/10	0.89/0.11	0.91/0.09	2.68[b]	1.16[b]
OH–$PV_{53}D_{537}$MS–OH	1/172/20	0.90/0.10	0.91/0.09	4.44[c]	–

[a] Determined by ^{1}H NMR.
[b] Absolute molecular weight: determined by MALLS.
[c] Calculated from apparent molecular weight.

of the HO–PV_lD_mMS–OH was determined by size-exclusion chromatography equipped with multiangle laser light scattering (SEC-MALS) analysis with a Shodex KF-806L column and a Wyatt Dawn HELEOS detector. The apparent molecular weights of the HO–PV_lD_mMS–OH were also measured using gel-permeation chromatography (GPC) through a Shodex KF-803 column using a calibration curve based on linear polystyrene standards. THF was used as the GPC solvent.

To obtain a macromolecular chain transfer agent (macro-CTA), DCC (4.0 molar to HO–PV_lD_mMS–OH) in CH_2Cl_2 (100 mL) was added dropwise to a CH_2Cl_2 (100 mL) solution of 4-cyanopentanoic acid dithiobenzoate (2.4 molar to HO–PV_lD_mMS–OH) and HO–PV_lD_mMS–OH (30 g) and stirred for 20 h at 40 °C (Scheme 2). The solution was then filtered to remove any insoluble substances. After evaporation of CH_2Cl_2, the reaction mixture was washed with methanol until the methanol was colorless, diluted with chloroform, washed three times with brine, dried over $MgSO_4$, and concentrated. A viscous liquid was obtained. The chemical structure of macro-CTA was confirmed by ^{1}H NMR (α-500, JEOL, Tokyo, Japan) and FT-IR spectroscopy (FT-500, Jasco, Tokyo, Japan). ^{1}H NMR (500 MHz, $CDCl_3$): δ = macro-CTA: −0.2 to 0.2 (m; Si–CH_3), 1.9 (s; CN–C–CH_3), 2.35–2.75 (m; –C–CH_2–CH_2–COOH), 5.6–5.8 (m; –CH=CH_2), 5.8–6.0 (m; –CH=CH_2), 7.3–7.9 (m; Ph).

2.2. Synthesis of block copolymers

Because the radical for polymerization was sensitive to air, all reactions were performed in an argon gas atmosphere. The synthetic condition of the block copolymers is summarized in Table 2. Typically, α,α′-azobisisobutyronitrile (AIBN, 0.025 mmol) was introduced through a polymerization tube. MPC (4.43 g, 15.0 mmol) and macro-CTA ($PD_{324}V_{32}$MS, 0.05 mmol) were desorbed in a toluene/ethanol (1/1) mixture, and the volume of the solution was adjusted to 30 mL. Then, argon gas was passed through the solution for 30 min to eliminate oxygen. The solution was heated at 70 °C and stored with gentle shaking for given periods. After polymerization, the block copolymer was precipitated into THF, then dissolved in ethanol, and again precipitated into THF. The precipitation was dried *in vacuo*. The synthetic route of the PMPC–PV_lD_mMS–PMPC triblock copolymers is shown in Scheme 3.

The number- and weight-averaged molecular weights of the block copolymers were measured with a Tosoh GPC system with a refractive index detector and size-exclusion columns, Shodex, SB-804 HQ and SB-806M HQ with a poly(ethylene glycol) (PEG, Tosoh standard sample) standard in 20 vol.% methanol containing 10 mM LiBr. The molar fraction of the MPC unit of block copolymer was also determined by phosphorus analysis.

2.3. Preparation of silicone substrate and surface functionalization

Silpot 184 PDMS prepolymer was mixed thoroughly with its cross-linking catalyst (10:1, w/w) and poured into a Petri dish. After the bubbles were removed from the prepolymer under reduced pressure, the films were cured at 100 °C for 3 h. The cured film was removed from the plate and cut into 1.4 cm diameter disks. The film disks were washed thoroughly with hexane

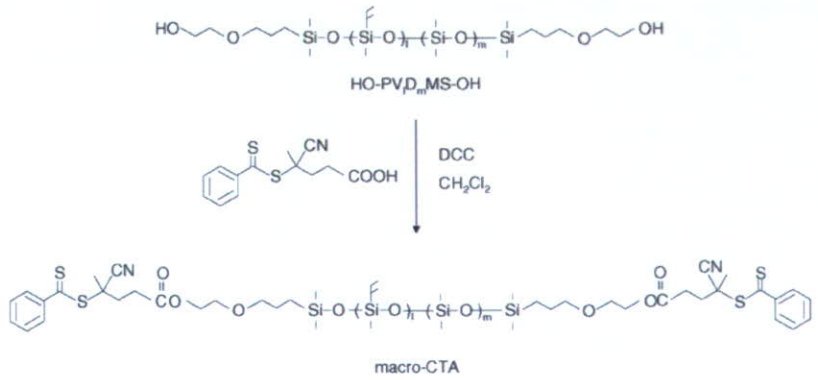

Scheme 2. Synthetic route of macro chain transfer agent (macro-CTA).

Table 2
Synthetic results of PMPC–PV$_l$D$_m$MS–PMPC triblock copolymers

Code	Copolymers	MPC/macro-CTA/AIBN (mol) in feed[a]	PMPC$_{PD(one\ side)}$ in copolymer[b]	M_w ($\times 10^4$)[c]	M_w/M_n	PMPC/silicone[d]
26–173	PMPC$_{26}$–PV$_{17}$D$_{173}$MS–PMPC$_{26}$	$1.5\times10^{-2}/1\times10^{-4}/5\times10^{-5}$	26.0	2.32	1.27	0.27
35–173	PMPC$_{35}$–PV$_{17}$D$_{173}$MS–PMPC$_{35}$	$1.5\times10^{-2}/5\times10^{-5}/2.5\times10^{-5}$	34.7	3.53	1.31	0.37
53–173	PMPC$_{53}$–PV$_{17}$D$_{173}$MS–PMPC$_{53}$	$1.5\times10^{-2}/2.5\times10^{-5}/1.25\times10^{-5}$	52.7	6.85	1.41	0.55
54–324	PMPC$_{54}$–PV$_{32}$D$_{324}$MS–PMPC$_{54}$	$1.5\times10^{-2}/1\times10^{-4}/5\times10^{-5}$	54.2	3.93	1.28	0.30
66–324	PMPC$_{66}$–PV$_{32}$D$_{324}$MS–PMPC$_{66}$	$1.5\times10^{-2}/5\times10^{-5}/2.5\times10^{-5}$	66.3	6.23	1.41	0.37
119–324	PMPC$_{119}$–PV$_{32}$D$_{324}$MS–PMPC$_{119}$	$1.5\times10^{-2}/2.5\times10^{-5}/1.25\times10^{-5}$	118.6	9.85	1.63	0.66
75–325	PMPC$_{75}$–PV$_{53}$D$_{537}$MS–PMPC$_{75}$	$1.5\times10^{-2}/1\times10^{-4}/5\times10^{-5}$	75.3	8.47	1.47	0.26
99–537	PMPC$_{99}$–PV$_{53}$D$_{537}$MS–PMPC$_{99}$	$1.5\times10^{-2}/5\times10^{-5}/2.5\times10^{-5}$	99.2	11.30	1.55	0.34
153–537	PMPC$_{153}$–PV$_{53}$D$_{537}$MS–PMPC$_{153}$	$1.5\times10^{-2}/2.5\times10^{-5}/1.25\times10^{-5}$	152.2	16.64	1.63	0.52

[a] [MPC] = 0.5 mol/L; [CTA]/[AIBN] = 2; polymerization temperature 70 °C; solvent: ethanol/toluene = 1/1 (v/v).
[b] Determined by phosphorus analysis, PD: polymerization degree.
[c] Determined by GPC, eluent: MeOH/H_2O = 20/80 with 10 mM LiBr.
[d] $n\times 2/(l+m)$, PMPC$_n$–PV$_l$D$_m$MS–PMPC$_n$.

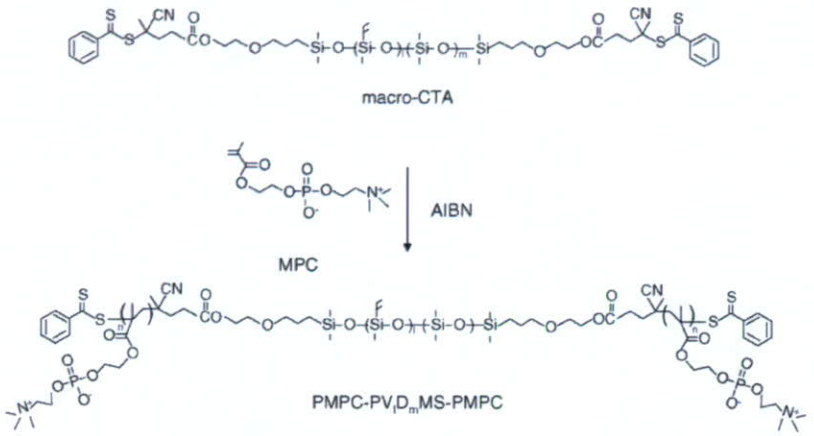

Scheme 3. Synthetic route of PMPC–PV$_l$D$_m$MS–PMPC triblock copolymer.

and acetone and dried under *in vacuo* for 1 day at room temperature. The surface functionalization of the PDMS films was processed as previously described [37]. Briefly, the silicone films were incubated in a solution of poly(hydromethylsiloxane) (KF-99-P®):2-propanol (3:5, v/v) containing triflic acid as a catalyst (0.02 mL) with stirring for 15 min at room temperature. The silicone films were then removed from the solution and washed thoroughly with 2-propanol and hexane, then dried *in vacuo* for 1 day at room temperature. The presence of surface Si–H groups (absorption peak at 2167 cm^{-1}) was confirmed by ATR-FT-IR.

2.4. Surface modification of silicone films with PMPC–PV$_l$D$_m$MS–PMPC triblock copolymer

A solution (5 g) of 1 wt% PMPC–PV$_l$D$_m$MS–PMPC triblock copolymers desorbed in ethanol was prepared and Pt-catalyst (platinum–divinyltetramethyldisiloxane complex) (two drops) was added to the polymer solution. The solution was dropped onto a Si–H functionalized silicone film and spin-coated at 4000 rpm for 10 s. The film was heated at 80 °C for 2 h, then rinsed by soaking in ethanol for 24 h at 50 °C. The ethanol was changed several times. The film was then dried *in vacuo*. Fig. 1 is a schematic representation of the surface modification of PDMS with PMPC–PV$_l$D$_m$MS–PMPC triblock copolymers.

2.5. Surface analysis

X-ray photoelectron spectroscopy (XPS) was performed on a Scienta ESCA-200 spectrometer with Al Kα. Survey scans

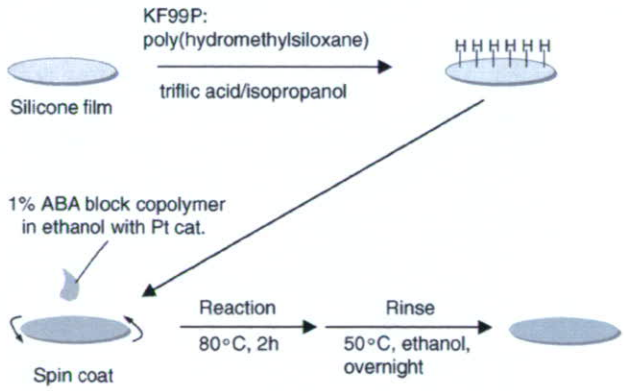

Fig. 1. Schematic representation of surface modification of PDMS with PMPC–PV$_l$D$_m$MS–PMPC triblock copolymer.

spectra of C 1s, O 1s, N 1s, and P 2p were obtained. All XPS data were collected at take off angles of 75° (between the specimen surface and the detector).

The dynamic contact angles for the samples were recorded as the probe fluid, water (deionized to 18.2 MΩ), using a First Ten Angstroms FT-125 goniometer and Gilmont syringes. The advancing (θ_A) and receding (θ_R) contact angles were measured with addition to and withdrawal from the drop, respectively.

The surface frictional coefficients during startup and under steady state conditions were measured using a surface property tester (Heidon Type32, Shinto Science Co., Tokyo, Japan). Sample films ($\phi = 1.4$ cm) were thoroughly wet with water before and during the measurements. The measurements were conducted by sliding the membrane under a 100 g load using a stainless steel ball (10 mm in diameter). The scan speed and scale were 10 mm/s.

2.6. Platelet adhesion test

Human platelet-rich plasma (PRP) was prepared from citrated whole blood by centrifugation. Polymer samples were placed in a 24-well tissue culture plate and secured with a silicone rubber ring. The PBS was allowed to stand in the wells overnight to equilibrate the surface. PRP was poured into each well and stored at room temperature for 60 min. The polymer surfaces in contact with PRP were observed by a scanning electron microscope (S-3400NX, Hitachi High-Technologies Co., Tokyo, Japan). The density of adherent platelets was determined by measuring lactic acid dehydrogenase (LDH) from the platelets [38]. After the PRP was incubated on the polymer samples, the samples were rinsed three times with PBS. The samples were then transferred to a new 24-well tissue culture plate. Triton X-100 (0.5 wt%, 1 mL) was introduced into each well and incubated for 30 min. The Triton X-100 solution (250 μL) was collected and the concentration of LDH from the adherent platelets was measured by the LDH-Cytotoxic Test kit (Wako Pure Chemical Industries, Ltd., Japan).

2.7. Controlled protein adsorption on surface patterned with UV-light irradiation

UV light ($\lambda = 185$ nm) (GL15ZH, Sankyo Denki Co. Ltd., 15 W) was irradiated on a poly(hydromethylsiloxane)-treated PDMS surface through a mesh used for transmission electron microscopy (hole 45 μm, bar 40 μm; Okenshoji Co. Ltd., Tokyo, Japan) for 3 h in air. The UV-irradiated surfaces were then immobilized with the triblock copolymer (119–324) mentioned above.

The surface was exposed to 0.45 g/dL fluorescein isothiocyanate (FITC)-labeled bovine albumin (Sigma Chemicals, St. Louis, MO, USA) in phosphate-buffered solution (PBS) for 30 min and rinsed with PBS and water. The sample was dried in an argon stream and observed using a fluorescent microscope (IX-70, Olympus Co., Tokyo, Japan).

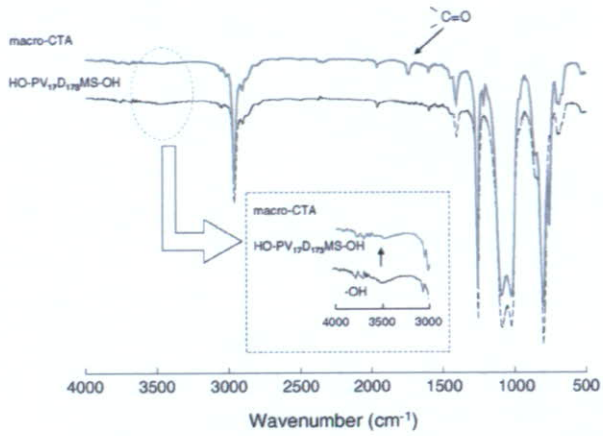

Fig. 2. IR spectra of $PV_{17}D_{173}MS$ and macro-CTA.

3. Results and discussion

3.1. Synthesis of triblock copolymers

Hydroxy-terminated poly(dimethylsiloxane) copolymers (HO–PV_lD_mMS–OH) were synthesized by ring-opening polymerization of cyclotetrasiloxane compounds (Scheme 1). The ratio of dimethylsiloxane and vinylmethylsiloxane in the copolymer could be controlled by their ratio in the feed. The molecular weight of the synthesized silicone compounds was measured by SEC-MALS. For HO–$PV_{17}D_{173}$MS–OH and HO–$PV_{32}D_{324}$MS–OH, the absolute molecular weights were $(1.43 \text{ and } 2.68) \times 10^4$, respectively. Their ratio of apparent molecular weight measured by GPC to absolute molecular weight was 1.4. The absolute molecular weight of HO–$PV_{53}D_{537}$MS–OH was calculated at 4.44×10^4 from the apparent molecular weight. The molecular weight of HO–$PV_{53}D_{537}$MS–OH increased linearly ($r^2 = 0.99$) with an increase in the monomer ratio to $M^R_2D_8$.

4-Cyanopentanoic acid dithiobenzoate, that is, the RAFT agent was reacted with the HO–PV_lD_mMS–OH by condensation. Fig. 2 shows the FT-IR spectra of HO–PV_lD_mMS–OH and that reacted with the 4-cyanopentanoic acid dithiobenzoate. After the reaction, absorption due to the carbonyl group at 1750 cm^{-1} was observed. The absorption of the hydroxyl group at 3500 cm^{-1} diminished. Quantitative determination of the condensation was performed by ^1H NMR. In every case, the composition of the RAFT agent was approximately 2 when the molecular weight of the silicone compound determined by SEC-MALS was used.

Living radical polymerization has a great deal of synthetic power in controlling the molecular architecture of polymers and is an exceptionally robust method for producing block or graft copolymers [28,39–41]. The living radical polymerization of MPC recently resulted in the preparation of biocompatible block [35,42–45] and graft copolymers [46,47].

While Ma et al. firstly synthesized a series of diblock and triblock copolymers of PMPC and oligodimethylsiloxane *via* ATRP, the characterization of the block copolymers was not described in detail because of the solubility

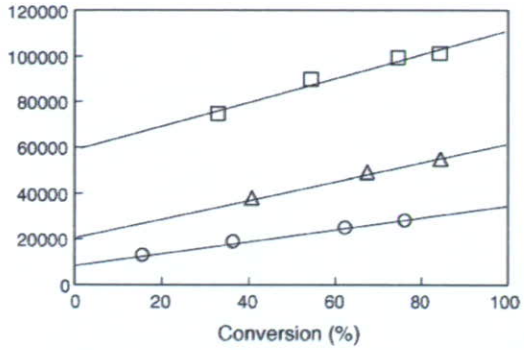

Fig. 3. Dependence of M_w on conversion in the polymerization of MPC: (○) PMPC–$PV_{17}D_{173}$MS–PMPC; (△) PMPC–$PV_{32}D_{324}$MS–PMPC; (□) PMPC–$PV_{53}D_{537}$MS–PMPC.

difference of the components [42]. We also tried to synthesize macro-initiator for ATRP. However, the decrease in the molecular weight of HO–PV_lD_mMS–OH was observed when HO–PV_lD_mMS–OH was reacted with 2-bromoisobutyryl bromide.

RAFT polymerization of MPC with RAFT agent-capped silicone as a dithioester chain transfer agent (macro-CTA) was then performed in toluene/ethanol (1/1) at 70 °C. Even though macro-CTAs have vinyl groups as side chains, any gelation during polymerization was not observed. Fig. 3 shows the relationship between the molecular weight determined by GPC and the conversion of the MPC polymers. In every polymer system, the GPC results show a single peak and the molecular weight of the block copolymer is linear with conversion. Fig. 4 shows that the monomer consumption followed first order kinetics. The semi-logarithmic plot indicates that polymerization is first order with respect to MPC and implies that the polymer radical concentration remains constant on the polymerization time scale. Table 2 summarizes the characterization of PMPC–PV_lD_mMS–PMPC triblock copolymers with various chain lengths. The degree of polymerization (PD) of the MPC polymer increased with an increase in the ratio of MPC to macro-CTA. The yield of polymerization related with polymerization kinetics and increased with an increase in the molecular weight of macro-CTA. The molecular weight distributions were relatively larger with the

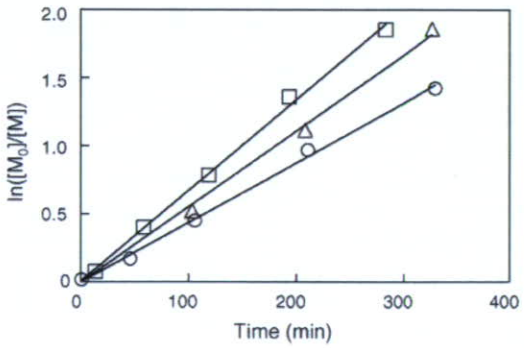

Fig. 4. Kinetics of RAFT polymerization of MPC: (○) PMPC–$PV_{17}D_{173}$MS–PMPC; (△) PMPC–$PV_{32}D_{324}$MS–PMPC; (□) PMPC–$PV_{53}D_{537}$MS–PMPC.

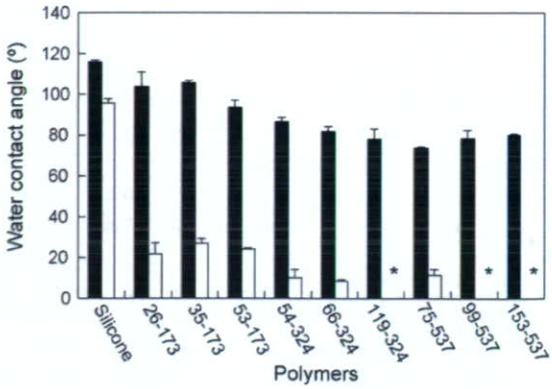

Fig. 5. Water contact angles of native silicone film and that coated with block copolymers: (■) advancing contact angle (θ_A); (□) receding contact angle (θ_R). * represents spreading of water drop.

higher molecular weights. The ratio of MPC and silicone units was calculated from the phosphorus analysis data. When $PV_{32}D_{324}$MS was used as macro-CTA, the composition of the MPC units in a copolymer was higher than that of other macro-CTAs.

3.2. Surface modification and characterization of PDMS with triblock copolymers

All copolymers were dissolved in ethanol and coated on silicone films. The water contact angle data was recorded using specimens dried for several hours under reduced pressure before measurement (Fig. 5). The data for the native PDMS was $\theta_A/\theta_R = 116°/96°$ and did not change by treatment with poly(hydromethylsiloxane). The θ_A on the surface coated with the triblock copolymers was recorded at the first addition of water and it gradually decreased with an increase in the composition of the MPC unit in the copolymers. The θ_R on the modified surface was decreased dramatically to less than 30°. Particularly, the θ_R on a surface coated with copolymers (119–324, 99–537, and 153–537) could not be measured because the water drop spread completely.

The elemental analyses of the polymer-coated silicone surfaces were performed with XPS. In the case of a silicone film coated with the triblock copolymer (66–324), nitrogen and phosphorus peaks were observed at 402.5 and 134.0 eV, respectively (Fig. 6). These were not observed on the native silicone film and were attributed to the phosphorylcholine group in the MPC units. To affect the chemical reaction of surface modification, the triblock copolymer was treated without a Pt catalyst or Si–H treatment. In both cases, the phosphorus and nitrogen signals caused by the MPC polymers were negligible. The surface modification with the triblock copolymers was then performed through hydrosilylation. The XPS phosphorus concentration of the surface-modified silicone films is summarized in Fig. 7. The increment of concentration was caused by an increase in the bulk composition of the MPC unit in the triblock copolymers. Although the block copolymer with a longer central silicone chain (153–537) has longer PMPC chains, the XPS phosphorus concentration on the surface coated with 153–537 was less